

Assessing subsurface transit times and denitrification in the Rock River Basin

GROUNDWATER SECTION, ILLINOIS STATE WATER SURVEY

VLAD IORDACHE, DANIEL B. ABRAMS, WALTON R. KELLY

Contents

Table of Figures	2
Introduction	4
Data sources	5
Water Quality Data	5
<i>IEPA Municipal Supply Records</i>	5
<i>ISWS PSL of domestic wells</i>	6
<i>IDOA Monitoring Wells</i>	8
Water Level data.....	9
Model description	11
Geography and geology	11
Temporal discretization	11
Water demand	12
Recharge and nitrate application.....	13
Artificial drainage.....	15
Denitrification	16
Model Calibration	17
Calibration to observed heads	17
Calibration to observed nitrate.....	18
Sensitivity Analysis: Denitrification	19
Results: Head, Concentration, and Age Maps	21
Head map.....	21
Discharge zones	22
Nitrate simulation	23
Groundwater age.....	26
Calculating Nitrate Loads	28
Future Directions	31
Acknowledgments	31
References	33

Table of Figures

Figure 1 Map of Rock River Basin. Large municipalities and locations of center pivots highlighted as potential sources of nitrate contamination.....	4
Figure 2 Selection of IEPA municipal water quality samples from sand and gravel [top] and bedrock [bottom] aquifer resources.....	6
Figure 3 Maximum shallow nitrate-N concentrations along the Rock River from 1980-1989 [Top] and 2005 to Present [Bottom]	7
Figure 4 Nitrate-N concentrations from 2000 to 2015 in Whiteside [Top] and Ogle/Lee [Bottom] Counties from IDOA water quality monitoring wells.....	8
Figure 5 Location of ISWS water level monitoring well network. Figure from (Burch, 2004).	9
Figure 6 Series of Sankoty aquifer potentiometric surfaces generated during peak pumping conditions in 1995, 2012, 2018, 2019, and 2020	10
Figure 7 Plan view of model geology in the shallow aquifer [Left], where yellow represents shallow sand and gravel aquifers and oranges/browns represent deeper clays and tills. Blue symbols represent the location of monitoring wells used for calibration. Plan view of the simulated groundwater flow regime in the shallow aquifer [Right], where reds are higher elevations and blues are lower elevations. Both images are from layer 4 [Tampico, unconfined aquifer].	11
Figure 8 Snapshot of pumping demands from all sectors during the summer of 2017.	12
Figure 9 Locations of center pivots in 2017 from: https://go.isws.illinois.edu/center-pivot-2017	13
Figure 10 Distribution of recharge zones throughout the model domain. See text for discussion.	14
Figure 11 Conceptualization of artificial drainage in the model. See text for discussion. Extensive Artificial Drain conceptualization includes the Artificial [Restricted] Drain conceptualization.	15
Figure 12 Model set up for simulating in-stream denitrification. Rates in the floodplain (orange) are 800 days, while the in-stream (red) rates are 600 days.	17
Figure 13 Observed vs simulated heads open to either the Tampico or Sankoty Aquifer.	18
Figure 14 Nitrate-N response in Whiteside County (195-3-80-1370) during variable seasonally applied recharge simulation.	19
Figure 15 Nitrate-N response in Lee County with varying levels of subsurface denitrification	20
Figure 16 Nitrate-N responses in Whiteside County, comparing the relative impacts of artificial drainage vs in-stream denitrification. Subsurface denitrification rates are assumed to be 1625 days everywhere in the model domain below layer 1.	21
Figure 17 Model generated potentiometric surface for the Tampico Aquifer near the GRLMN. Blue crosshairs symbolize the locations of individual monitoring wells/calibration points.....	22
Figure 18 Plot of vertical flow [Qz] in ft/day in layer 2. Regions with negative flow directions [green] are interpreted to be discharge zones, while regions with positive flow directions are interpreted to be regions of aquifer recharge.....	22
Figure 19 Drain outlet along the Green River, south of Prophetstown. Untreated discharge from fertilized fields can short-circuit denitrification zones and discharge directly into surface water.	23
Figure 20 Model generated nitrate-N concentration [mg/L] distribution after Stress Period 1 [1980 non-irrigation], Layer 4 [Tampico aquifer]	24

Figure 21 Model generated nitrate-N concentration [mg/L] distribution for Stress Period 50 [2004 irrigation], Layer 4 [Tampico aquifer]. Black line is the location of the bottom cross section. 25

Figure 22 Model generated nitrate-N concentration [mg/L] distribution for Stress Period 101 [2030 non-irrigation], Layer 4 [Tampico aquifer]. Black line is the location of the bottom cross section. 26

Figure 23 Model generated groundwater age distribution at end of simulation [Stress Period 101], Layer 2. Black line is the location of the bottom cross section. The deepest shade of red represents water that is 50 years of age or older. 27

Figure 24 Model generated groundwater age distribution at end of simulation [Stress Period 101], Layer 9. Black line is the location of the bottom cross section. 28

Figure 25 Mass balance polygons used in nitrate load calculations. 29

Figure 26 Nitrate-N response in Whiteside County (195-3-80-1370) during variable seasonally applied recharge simulation with triple nitrate-N inputs compared to baseline (Figure 14)..... 30

Introduction

To investigate the contributions of groundwater to increasing nitrate loads in the Rock River Basin (Figure 1), the Illinois State Water Survey [ISWS] has been tasked by the Illinois Environmental Protection Agency [IEPA], to construct a groundwater flow model that simulates subsurface and in-stream denitrification and groundwater to stream discharge regimes in the region. This report summarizes the findings of that effort.

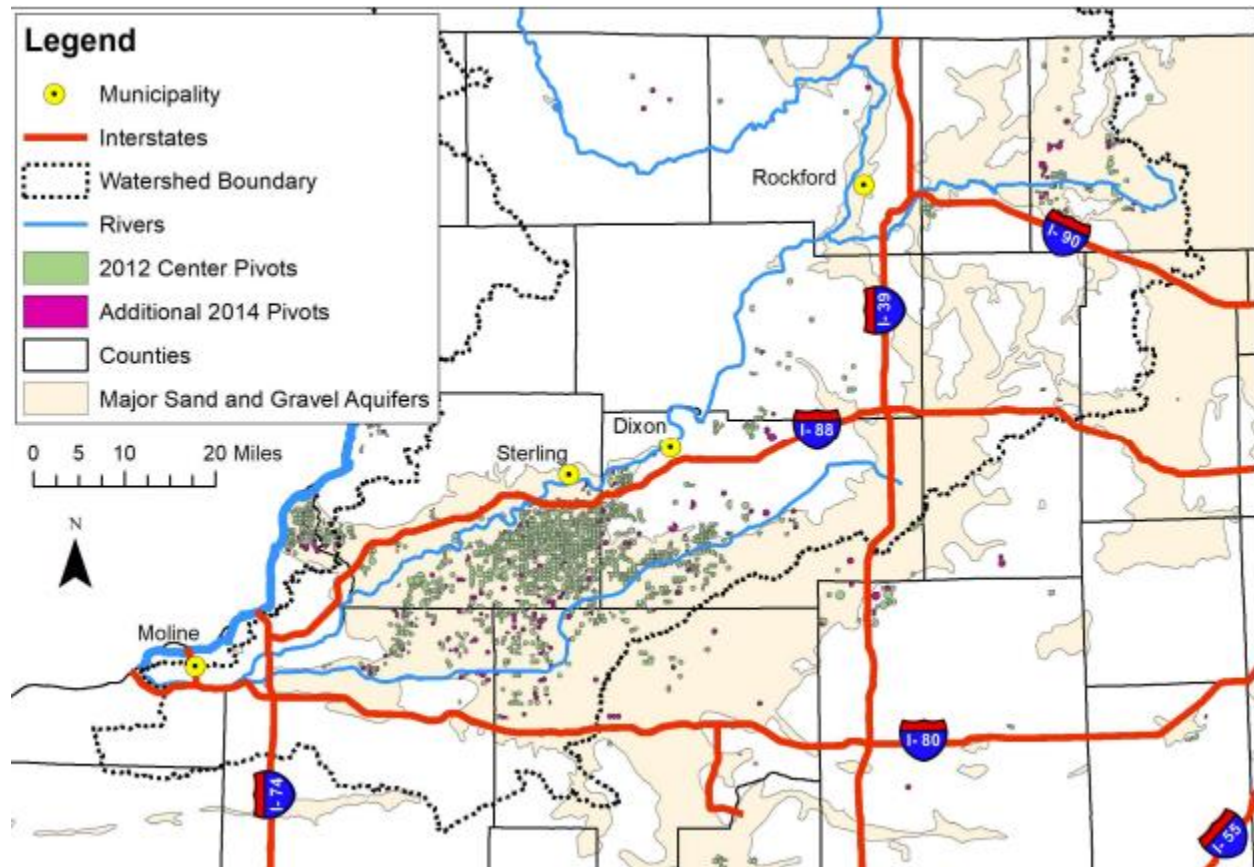


Figure 1 Map of Rock River Basin. Large municipalities and locations of center pivots highlighted as potential sources of nitrate contamination.

Nitrate-nitrogen (nitrate-N) loads to the Illinois portion of the Rock River have nearly doubled from a baseline period (1980-96) to the modern day (2013-2017) (Mclsaac, 2019). Determining the cause of this increase is confounded by numerous interconnected variables including changing climate, land use, and management strategies. Legacy nitrate in groundwater was identified as a potential explanation for the remaining increased nitrate load that could not be accounted for by increased irrigated acres, increased acres of corn and soybeans, reduced in-stream denitrification, increased population and measurement errors (Mclsaac, 2019).

Although simulations of groundwater age lend support for the hypothesis that contaminants can be held in the subsurface for decades before discharging to rivers, and that nitrate contributions from groundwater can increase as a result of increasing input from agricultural land use, the simulated increase in contribution is an order of magnitude less than what is required to explain the observed

increases in the Rock River. Two observations provide possible explanations for the small increase in groundwater delivery of nitrate. First, a regionally extensive aquitard (Burch, 2004) prevents appreciable nitrate from reaching the lower, older Sankoty aquifer. This suggests that the predominant source of groundwater nitrate comes as seasonal inputs from the thinner, unconfined, younger Tampico aquifer. Additionally, observed depths (Kelly & Ray, 1999) and rates (Puckett et al., 2011) (even under the most conservative considerations) suggest that subsurface denitrification occurs too near the surface and too quickly to allow for effective legacy accumulation in the dominant aquifers of the study region. This is especially true in model simulations that considered additional zones of “in-stream” denitrification near and within river cells (Puckett et al., 2011).

The role of artificial drainage in nitrate delivery to the Rock River merits further consideration. Drain tile and other stormwater control structures circumvent the potential for impoundment of nitrate contaminated water in the subsurface and decreases the time available for denitrification to occur. In addition, the reductions in recharge to groundwater associated with tile drain installation should theoretically decrease the discharge rates of older groundwater to the Rock River.

Data sources

Water Quality Data

Water quality data for the region has been compiled from three sources: IEPA municipal supply records, ISWS Public Service Lab [PSL] domestic well records, and Illinois Department of Agriculture [IDOA] dedicated water quality monitoring well network records.

IEPA Municipal Supply Records

A selection of time series for municipal supply data is shown in Figure 2. While some shallow wells in the IEPA database had no or undetectable nitrate-N concentrations, elevated concentrations occurred in Ogle (Figure 2; Ctry Est Subd 2) and Whiteside (Figure 2; Erie 2) Counties. Seasonal variability, in nitrate-N concentrations, is captured and expected in this dataset. What is surprising is the magnitude of variability in some instances, and that the variability is occurring at great depth (Leaf River 3, Byron 3, Lakeview Hills 2). Other wells (Rolling Green Est 1) show a well-defined, increasing trend in concentration. The rate and magnitude nitrate-N concentration change is highly variable, indicating that the pathways for contaminant travel and removal are complex and vary spatially. Most striking is the increase at Byron 3, where a well at 715 ft depth has an increasing nitrate-N concentration from 2 to 6 mg/L, and then returns to baseline levels over the next few years. While nitrate-N concentrations in water from deep bedrock sources is important to monitor from a drinking water supply perspective, peak concentrations are at least half of baseline concentrations from shallower sources. Furthermore, since nitrate can only enter the model through recharge, insufficient time is available to accumulate nitrate at these depths during simulation.

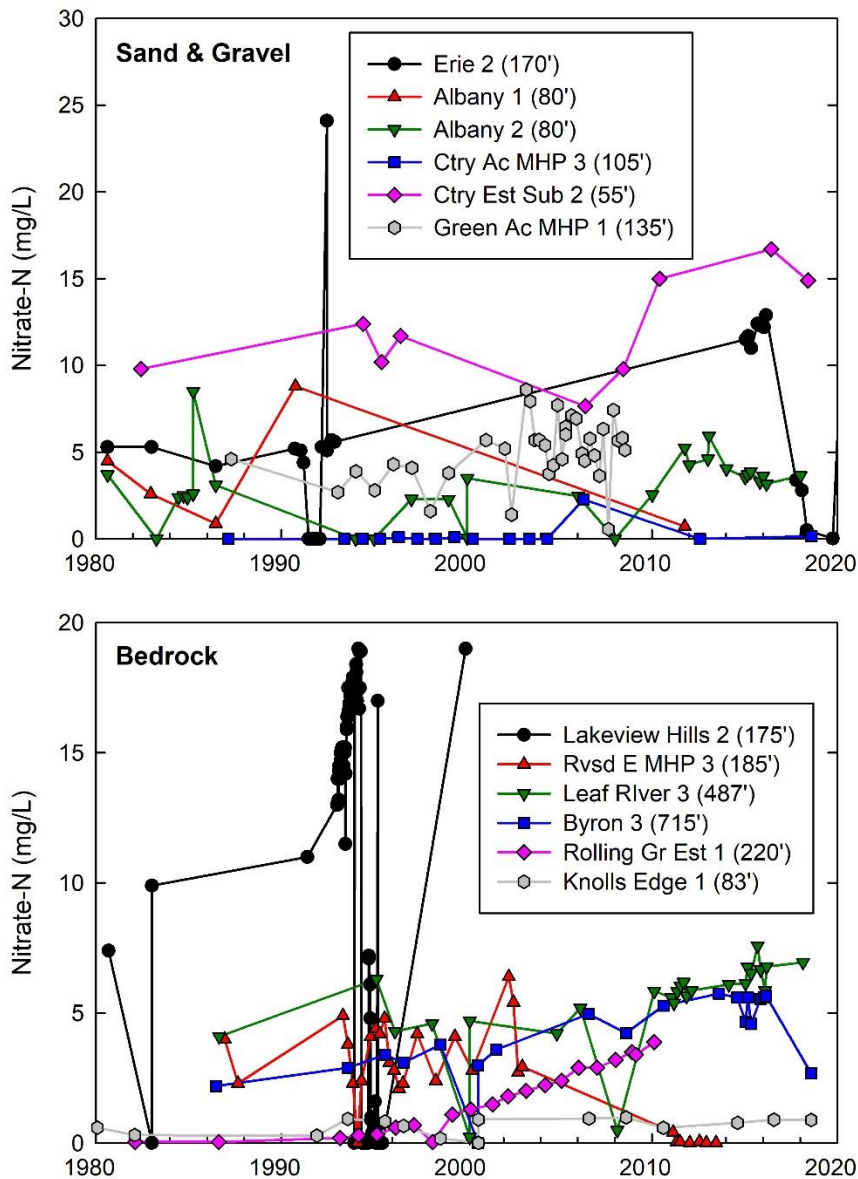


Figure 2 Selection of IEPA municipal water quality samples from sand and gravel [top] and bedrock [bottom] aquifer resources.

ISWS PSL of domestic wells

While municipal demands and therefore water quality analyses are primarily sourced in deeper aquifers, shallow unconfined aquifers play a more significant role in mediating nitrate contaminant transport to rivers and streams. To bolster nitrate data in the shallow aquifers, which is the focus of this modeling study, ISWS PSL records of domestic wells [which tend to be shallower] were incorporated into the data model as well (Figure 3).

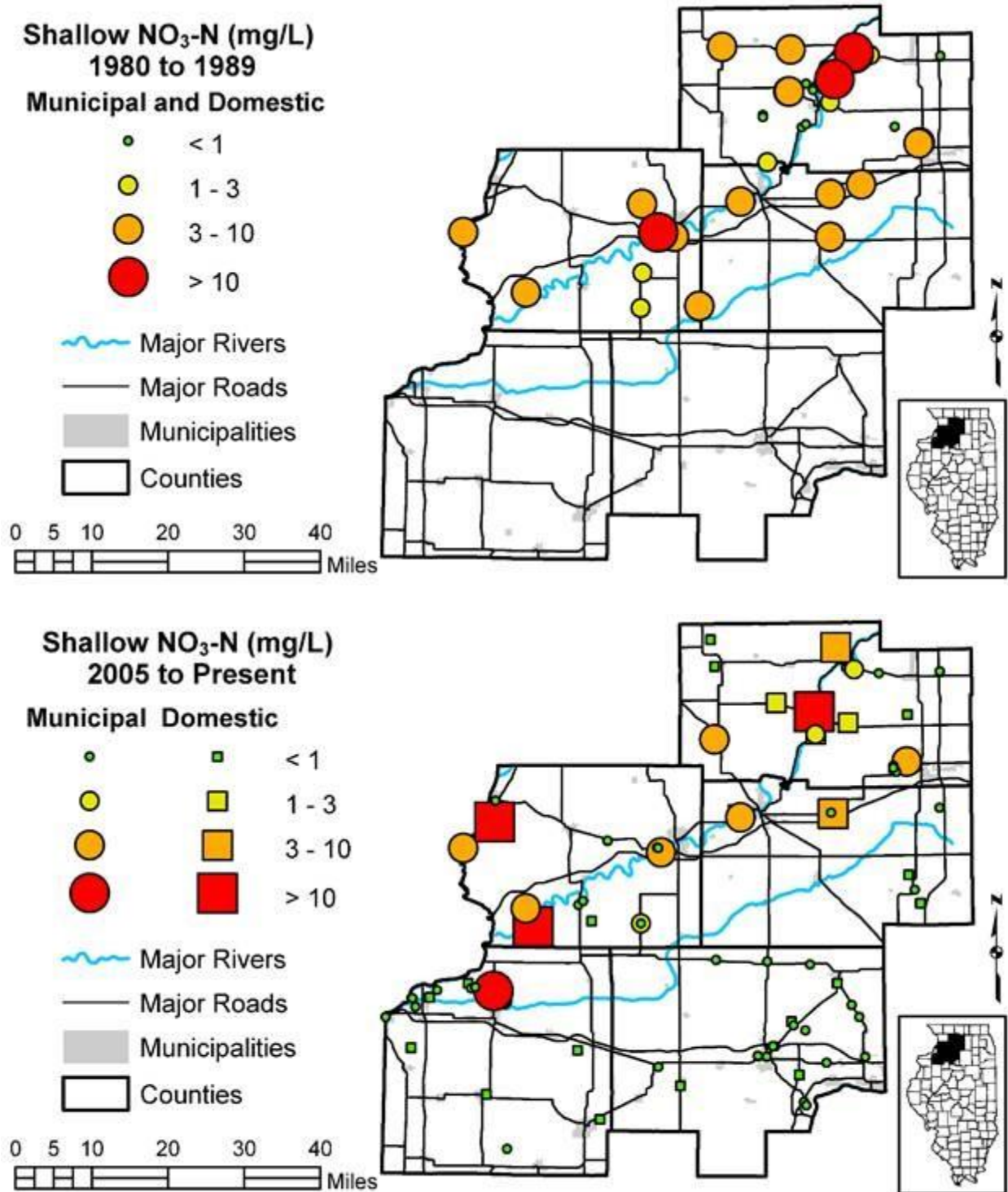


Figure 3 Maximum shallow nitrate-N concentrations along the Rock River from 1980-1989 [Top] and 2005 to Present [Bottom]

While the domestic well data provides better spatial coverage, wells are not sampled as frequently as municipal wells. As a result, it is difficult to discern exactly how the nitrate-N concentrations in the aquifer shown in Figure 3 are changing over time. However, these data are highly suitable for purposes of the model, as they can be used as targets in the specific season of the year that they were measured (the transient model is broken up into seasons to accommodate this information).

IDOA Monitoring Wells

IDOA maintains a network of groundwater quality monitoring sites throughout the State, and we have access to their complete nitrate records from 2000 through 2015. This source of data is particularly valuable because it is primarily sourced in the shallow aquifers, and samples were collected regularly (every few years).

The existing dataset suggests that nitrate-N levels in shallow groundwater are not increasing through time. In fact, in 6 out of 10 wells presented in (Figure 4), nitrate-N levels decreased during the period of record. The other 4 stayed the same or had undetectable nitrate-N throughout.

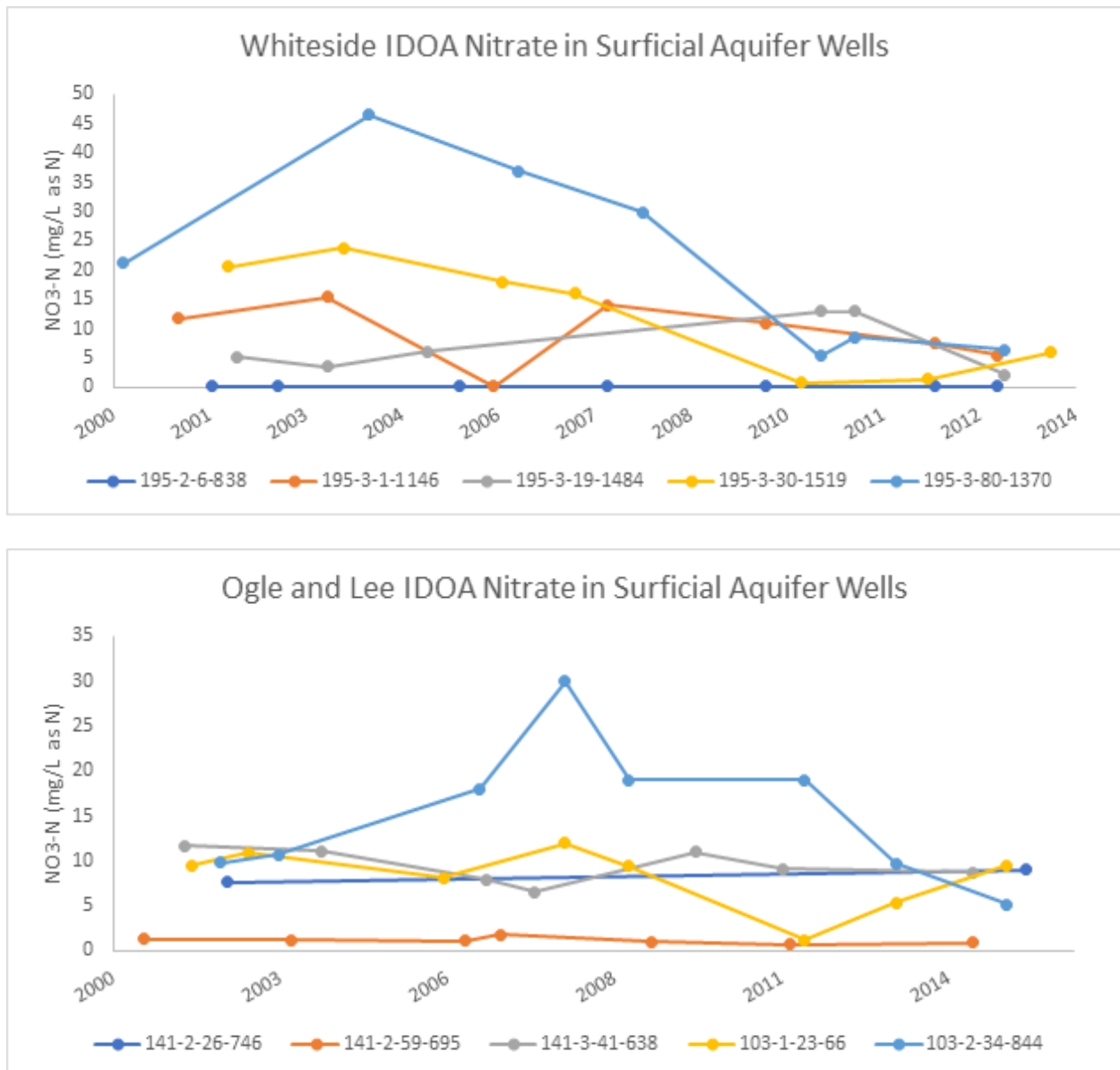


Figure 4 Nitrate-N concentrations from 2000 to 2015 in Whiteside [Top] and Ogle/Lee [Bottom] Counties from IDOA water quality monitoring wells.

Although the IDOA dataset is the most useful for this study, there are still aspects of nitrate flow through groundwater that cannot be confidently accounted for. Repeat quarterly and monthly measurements at individual wells along the Upper Illinois River (Lin et al., 2019) reveal a strong seasonality in nitrate-N

concentrations in addition to variability in the dominant input source (urban sewage vs. agriculture runoff) based on isotopic analysis. Without a similar campaign in this region, no reliable statements can be made regarding seasonality or input source.

Water Level data

Understanding the spatial variability of water levels in an aquifer through time is a critical component in model development. Fortunately, ISWS has maintained a water level monitoring well network in the Rock River Region for over 30 years (Figure 5).

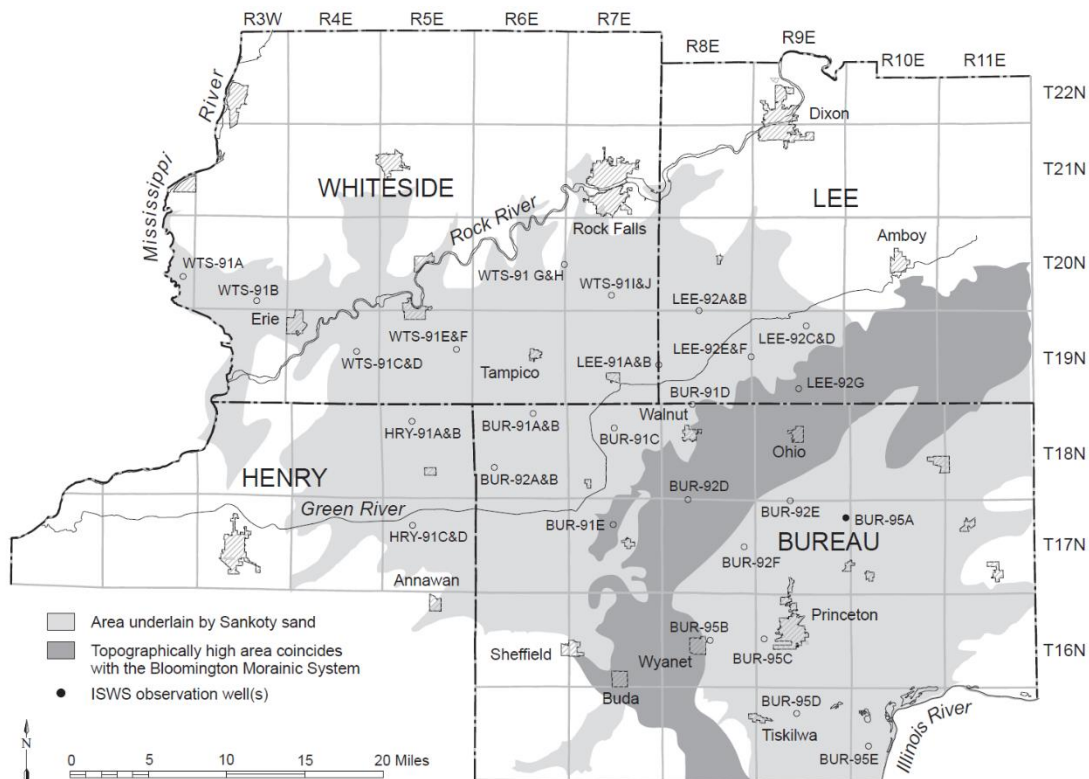


Figure 5 Location of ISWS water level monitoring well network. Figure from (Burch, 2004).

Detailed information regarding the network itself, access to view and download the entire period of record, and summary of the region’s groundwater hydrology can be found at the following webpage: <https://aqueduct.isws.illinois.edu/grl-monitoring.html>.

Water levels from the Green River Lowlands Monitoring Network [GRLMN] form the primary calibration targets for the current flow model. Additionally, pumping demands are reported on an annual basis from Public and Industrial high capacity water users. Having sub-annual water level data will allow for apportionment of annual demands into a transient model as well as provide constraints on spatial demand estimates for sectors where annual reporting compliance is low. For example, agricultural irrigation. Even though ISWS receives occasional annual reports from only 10% of the known agricultural entities who utilize center pivot irrigation in this region, GRLMN allows us to monitor the effects of increasing irrigation demands through time and make reasonable estimates about the timing and quantity of the remaining 90% of demands that go unreported.

The peak demand [August for this region] potentiometric surfaces generated with monitoring well data (Figure 6) show that shortly after the network was established (1995), dry summers did not generate as observable irrigation demands as wetter summers do today (2018 – 2020). This is the result of an explosion of center pivot installation in response to the most recent drought (2012), especially in northwest Bureau County where the confining layer is thickest.

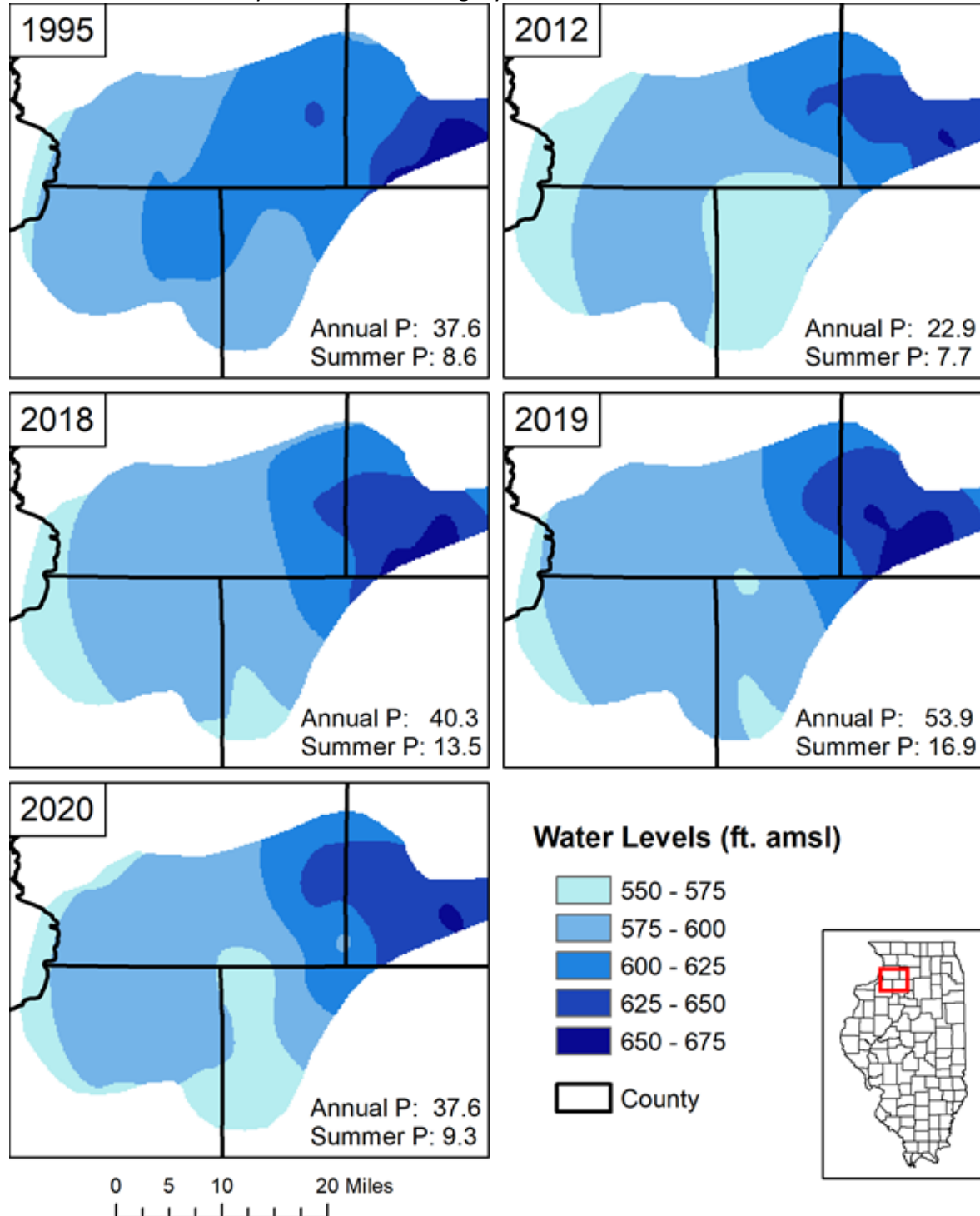


Figure 6 Series of Sankoty aquifer potentiometric surfaces generated during peak pumping conditions in 1995, 2012, 2018, 2019, and 2020

Model description

Geography and geology

The groundwater flow model used for this study is based off the MODFLOW model developed for the northern half of Illinois, detailed in ISWS Contract Report 2018-04 (Abrams et al., 2018). To reduce run-times, the model was trimmed to the northwestern portion of Illinois, as shown in . The model is ten layers, with the upper nine representing highly permeable unconsolidated sands and gravels (yellow areas in Figure 7 [Left]) but also low permeable tills and clays (orange and brown areas in Figure 7 [Left]). The tenth layer represents the material located at the bedrock surface, which ranges from low permeable shales to higher permeable dolomites and sandstone. Major surface water features in this model include the Rock, Mississippi, Illinois, and Green Rivers. These are represented by river cells, which can both add or remove water from an aquifer depending on the hydrogeologic conditions and stresses on the aquifer. Low permeable material and low order streams are represented by drain cells, which can only remove water from an aquifer.

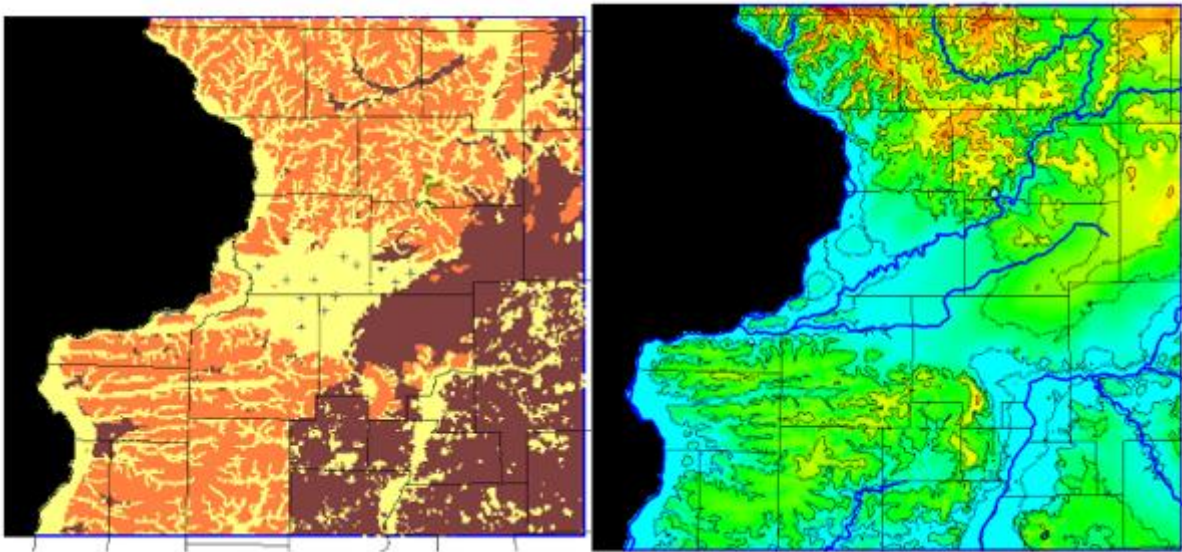


Figure 7 Plan view of model geology in the shallow aquifer [Left], where yellow represents shallow sand and gravel aquifers and oranges/browns represent deeper clays and tills. Blue symbols represent the location of monitoring wells used for calibration. Plan view of the simulated groundwater flow regime in the shallow aquifer [Right], where reds are higher elevations and blues are lower elevations. Both images are from layer 4 [Tampico, unconfined aquifer].

The pre-development (equilibrium conditions, without pumping) flow regime of the upper unconfined aquifer are shown in Figure 7 [Right]. North of Lee County groundwater gradients (in excess of 100 ft/mile), and therefore transport rates, are high, while gradients significantly flatten throughout the Green River Lowlands region (less than 2 ft/mile) (Burch, 2004).

Temporal discretization

The transient model starts in 1950 and runs through 2030. The temporal domain is broken up into 101 Stress Periods (SP). SP1 is 30 years and is run to steady state conditions to define initial conditions for the rest of the model. After SP1, the model alternates between 90-day irrigation stress periods and 275-day non-irrigation stress periods. We defined pumping and recharge rates in the model for the specific period represented by each stress period.

Water demand

Water demand (Figure 8), and withdrawal locations from Public Supply and Industrial sectors were obtained from annual reports submitted to the Illinois Water Inventory Program (IWIP) and imported into the model.

Self-reported annual withdrawals to IWIP were insufficient to characterize true demands in the agricultural sector. An ISWS web-map (Figure 9), which tracks Illinois, center pivot installation in 2012, 2014, and 2017, was used to scale mean, IWIP-reported, gallons of water withdrawn per acre, to the actual number of center pivot irrigated acres present in a given county. 2017 was used as a benchmark year because it had the highest statewide reporting percentage of the 3 years available. For example, in Whiteside County, IWIP can account for the water demand on 5,275.27 acres out of the 66,808.01 acres that were present in 2017 [~8%]. On average, ~75,000 gallons of water withdrawn per acre was reported. This rate was applied to the remaining center pivots in proportion to the number of acres an individual pivot occupies. This procedure was attempted to be applied to the remaining counties in the model domain. However, there were 7 counties in which irrigation pivots were found, but no reported 2017 IWIP data exists. In those cases, the mean of the mean withdrawal rate of adjacent counties with available data was used.

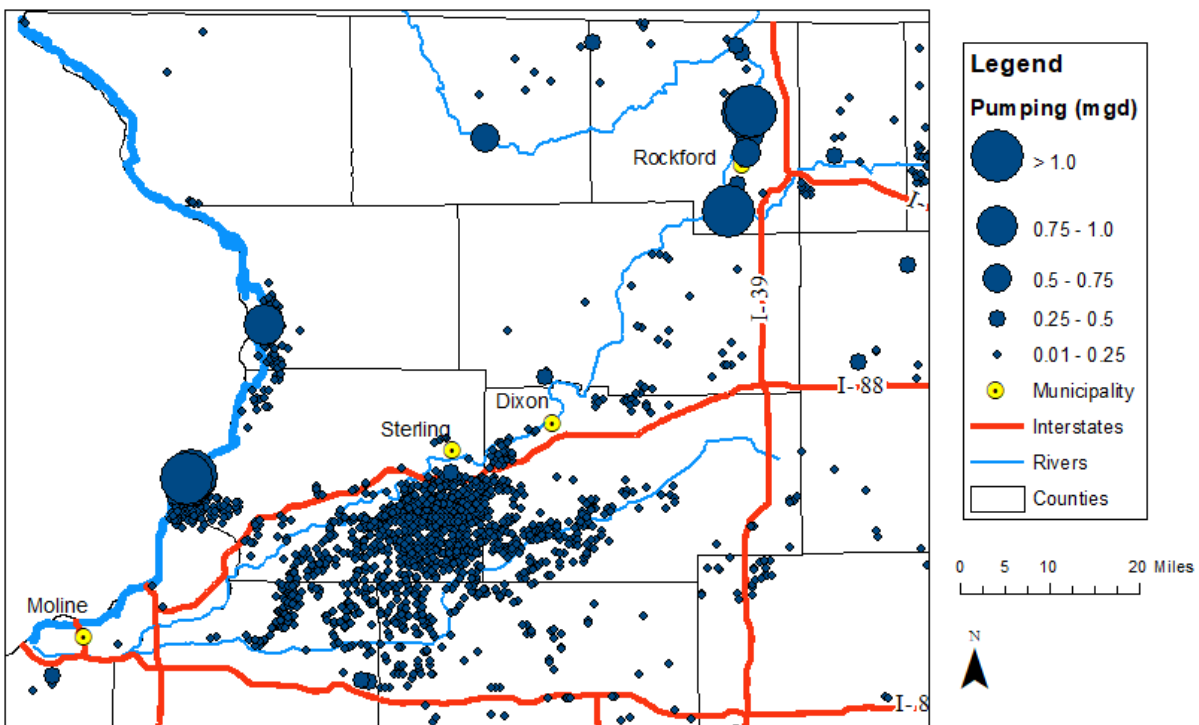


Figure 8 Snapshot of pumping demands from all sectors during the summer of 2017.

The percent increase in irrigation pivot acres from 2012 to 2017 was also calculated for each county, assumed to be constant, and used to forecast demands into the future as well as backcast to 1980. Model-wide, irrigated acres increase by ~5% every 3 years.

Center pivot locations in 2017 (Figure 9) were taken to be withdrawal point locations for agricultural water demand and were assumed to be in Layer 9. This assumption is broadly correct for the region, but especially near the Rock River in Whiteside and Lee Counties, where Layer 9 represents the Sankoty Aquifer and farmers generally do not run multi-pivot irrigation wells. Rather than adding or removing withdrawal points from the model with increasing or decreasing stress periods, withdrawals were adjusted at all withdrawal points following the criteria described in the previous section. Given the resolution of our model and the relatively short time domain in which the model runs, this simplification does not have a major influence on the simulated transport of nitrate.

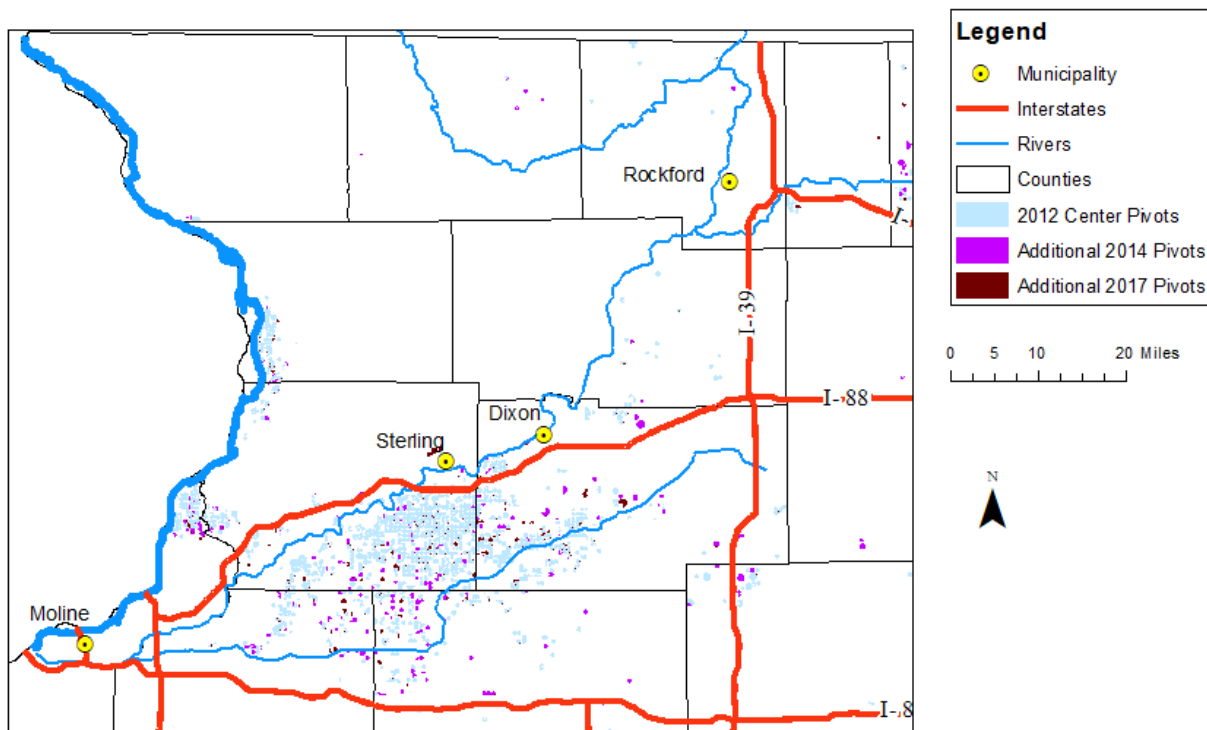


Figure 9 Locations of center pivots in 2017 from: <https://go.isws.illinois.edu/center-pivot-2017>

Recharge and nitrate application

During SP 1, a homogeneous areal recharge that had a nitrate-N concentration of 5 mg/L was applied. This allowed for an initial accumulation of nitrate in groundwater under the influence of predevelopment flow regimes. SP 2 represents the summer of 1980 in which the first estimated agricultural irrigation demands occurred. Subsequent odd Stress Periods represent the portions of a year without agricultural irrigation demand, while subsequent even Stress Periods represent the part of a year with agricultural irrigation demand. The final Stress Period [101] is the part of the year 2030 in which agricultural irrigation demands were not simulated.

Artificial drainage

During the study period, the role of artificial drainage was identified as a variable that merited further consideration. Prior to utilization of the Green River Lowlands region for agricultural production, the landscape was closer to that of a sandy wetland with low relief (Worthen, 1866). Extensive drain tiling was necessary to drain the landscape initially and is still necessary to protect yields during flood conditions, and lower the water table in Spring to facilitate planting. To incorporate this variable into the model, two tile drain infrastructure conceptualizations (Figure 11) were constructed from information from a previous study (Valayamkunnath et al., 2020).

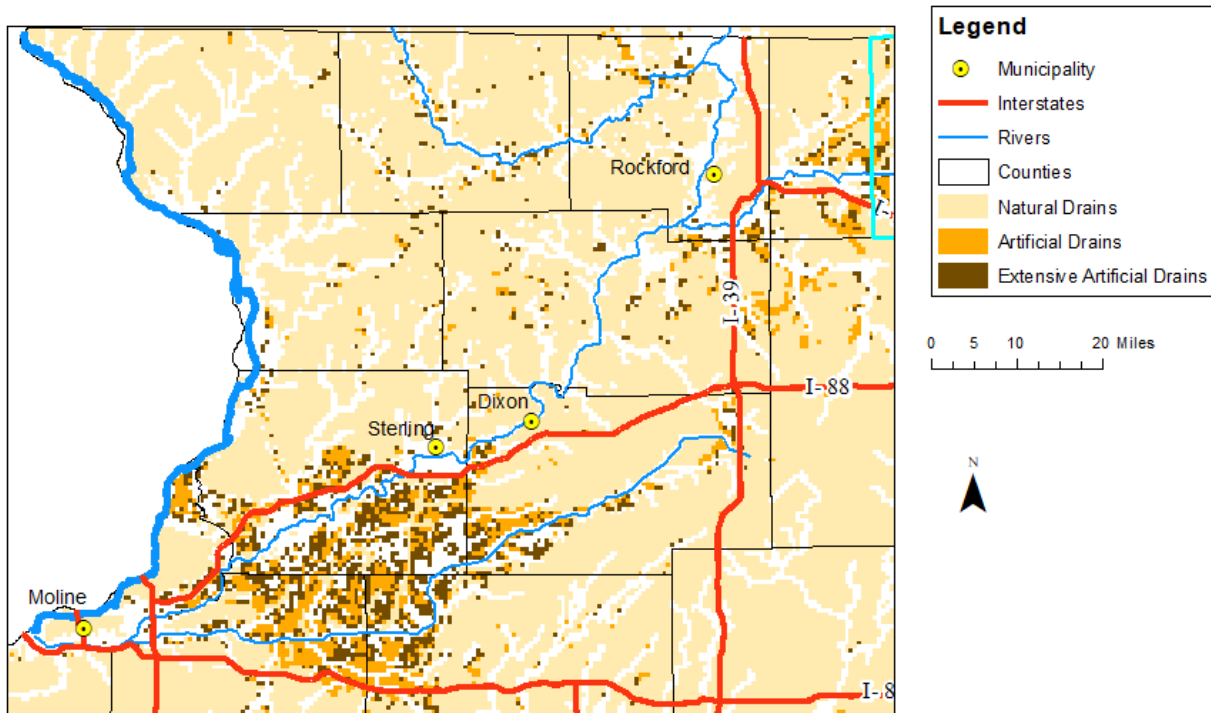


Figure 11 Conceptualization of artificial drainage in the model. See text for discussion. Extensive Artificial Drain conceptualization includes the Artificial [Restricted] Drain conceptualization.

This study correlated county-scale, self-reported, drain tiled acres to the 2017 USDA Census of Agriculture and 2016 National Land Cover Database GIS coverages, with 30 meter resolution information on soil-type (SSURGO v2.0) and slope (SRTM-DEM) to assign tiled acres to their most-likely spatial location. The resulting GIS coverage was validated with over 16,000 data points derived from aerial imagery. Accuracy was approximately 88% over the Midwest United States (Valayamkunnath et al., 2020).

The first conceptualization assumed that if at least 50% of a model cell was predicted to have drain tiles, then the cell was reassigned as a drain. This conceptualization was termed the “restricted” tile drain setup, because isolated patches of drain tile exist that do not readily communicate with rivers. The second setup assumed that if at least 25% of a model cell was predicted to have drain tile, then the cell

was reassigned a drain. This conceptualization was termed the “extensive” tile drain setup, to distinguish it from the “restricted” model.

An important note on tile drains. In a regional groundwater flow model, each cell can be assigned as a drain boundary condition cell if appropriate. Drain cells can remove water from an aquifer, but they are unable to add water. They are also assigned a conductance value that introduces a resistance to flow in the model; in our model, drain conductance was set at 1600 ft²/d. The effect of the drain is smeared over the cell; it is not treated as a discrete feature in MODFLOW. As a result, regional averaging over the cell resolution (2500 ft) is anticipated; local impacts might be more prominent.

Denitrification

Simply stated, denitrification is the anaerobic process by which aqueous nitrate is converted to gaseous nitrogen or a reduced oxide of nitrogen (NO, N₂O, etc.). This removal mechanism limits the amount of nitrate available to discharge to surface water. This model considers denitrification in two regimes. The first is within the subsurface. Layers 2 and below in the model are considered to be reducing environments. This designation is somewhat arbitrary, since redox conditions, and therefore the depth at which denitrification occurs, of the aquifer can be highly variable spatially and temporally. A previous ISWS study (Kelly & Ray, 1999) that assessed subsurface nitrate-N concentrations in Mason County, Illinois, suggested that depths of 20-30 feet is where redox or biological conditions strongly favor denitrification. Where the sands and gravels underlying the Rock River watersheds are thickest, this depth is roughly coincident with the thickness of layer 1. A detailed sampling plan will have to be employed to better capture the heterogeneity and seasonality of subsurface denitrification. This study focused on the regional effects of uniform rates over time in order to simulate average conditions.

The other denitrification regime considered was near (a proxy for the floodplain) and within river cells (Figure 12) in layer 1, which are considered to be zones of high organic content with rapid denitrification rates (Forshay & Stanley, 2005).

Two of the major controls on the rates of denitrification are local redox conditions and percent organic content. A survey of published literature revealed a large range of measured nitrogen removal rates (expressed in half-lives). Organic-rich, oxygen-poor environments can have half-life removal rates as fast as 500 days, while organic-poor, oxygenated environments have much slower removal rates around 2750 days (Uffink, 2003). Values in excess of 15,000 days were also observed in a study (Puckett et al., 2011), but it was more practical to model this as assuming no denitrification at all, considering the time domain of the model. True denitrification rates within the model domain are uncertain and have likely changed historically with new climate and land-use scenarios. For this study, both extremes are modeled to assess the range of possible outcomes. The median value (1625 days) was chosen as the base case simulation, because there are no field studies or justification to favor either extreme.

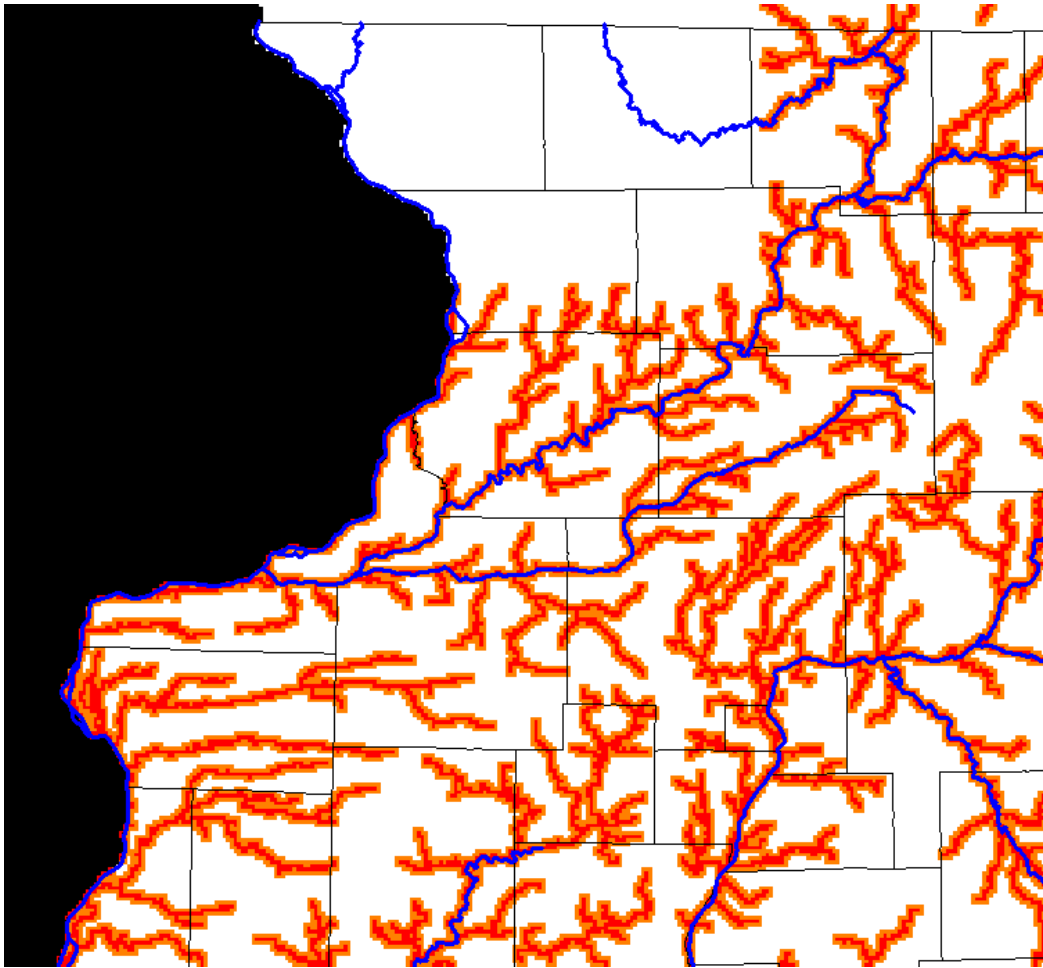


Figure 12 Model set up for simulating in-stream denitrification. Rates in the floodplain (orange) are 800 days, while the in-stream (red) rates are 600 days.

Since the model cells are larger than the scale of most studies regarding in- and near stream denitrification (Puckett et al., 2011), and those studies indicate extremely rapid rates of denitrification over short distances it was decided to use rates near the fastest observed extremes (~500 day half-life), but a little slower (800 flood plain, 600 in-stream) to account for the distance discrepancy.

Model Calibration

Calibration to observed heads

The groundwater flow model was calibrated to dedicated observation wells completed in either the Tampico or Sankoty aquifer (Figure 13). All observed data points were considered, and heads could fluctuate by a few feet within a stress period. In the Tampico the variability is largely driven by changes in recharge; in the deeper Sankoty the variability is driven by pumping demands, particularly during the irrigation season. As a result, the root mean square error of the data are considerable (3.0 ft for the Tampico and 6.0 ft for the Sankoty). In contrast, the mean error is closer to zero (-0.6 ft for the Tampico and 1.3 ft for the Sankoty). Further, the simulated data are strongly correlated to the observed data in the Tampico ($R^2 = 0.97$). The correlation is weaker in the Sankoty ($R^2 = 0.79$), which follows from the

variability in summertime heads. To improve calibration, more information would be needed regarding seasonal pumping demands; however, our sensitivity analysis indicates that varying pumping in the Sankoty had only a minor impact on nitrate simulations.

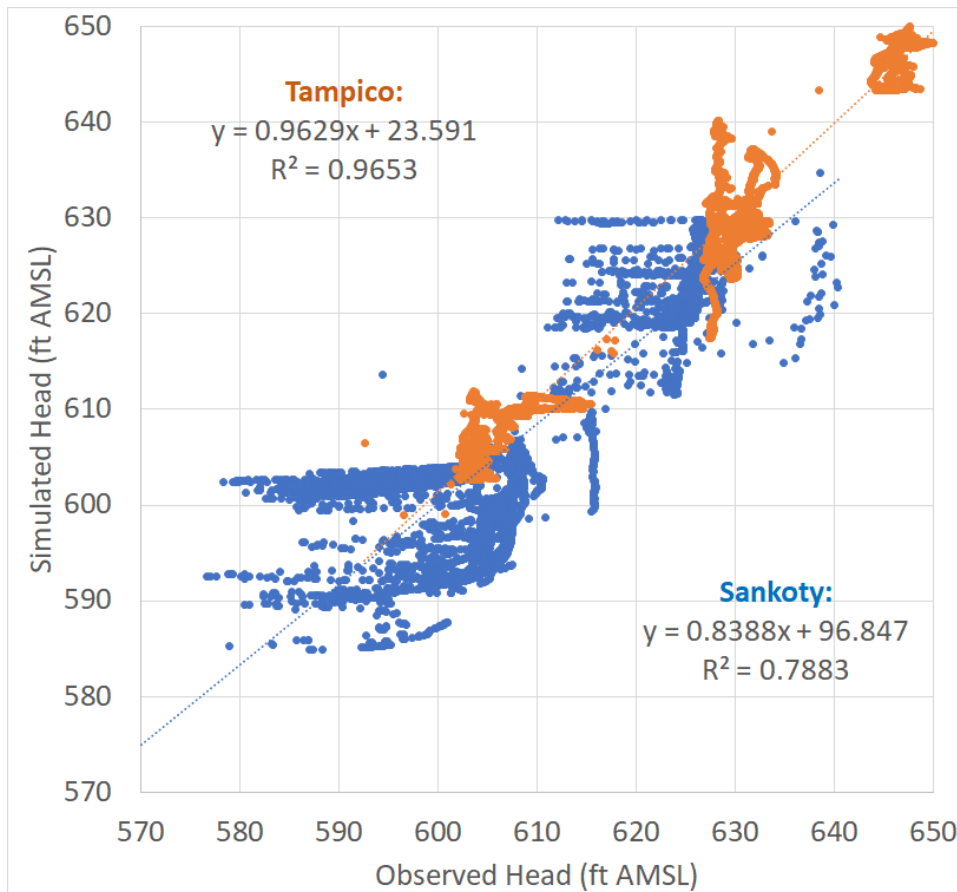


Figure 13 Observed vs simulated heads open to either the Tampico or Sankoty Aquifer.

Calibration to observed nitrate

Calibration to nitrate-N is challenging, primarily because the targets are of unknown quality. Frequently there are variations that are not normally observed in contaminants entering groundwater, and there is a good chance that some target points in the model may be due to flawed measurement. It is also possible that the targets represent very strong temporal and spatial variability. In a few instances, nitrate-N was observed above the EPA primary standard of 10 mg/L and below the detection limit in two nearby wells with similar open intervals. Our calibration approach focused on a well-by-well basis and attempted to capture the average condition through time (Figure 14); attempts to calibrate to seasonal fluctuations in nitrate applications did not yield the same variability as in some of the observations. To build confidence in the calibration as anything other than representative of average conditions, we would need a detailed sampling plan. These ideas are discussed in more detail in other sections of this report.

Without additional data collection, the model is best utilized as a tool for understanding the subsurface and evaluating the regional long-term impacts of increases or decreases in nitrate applications.

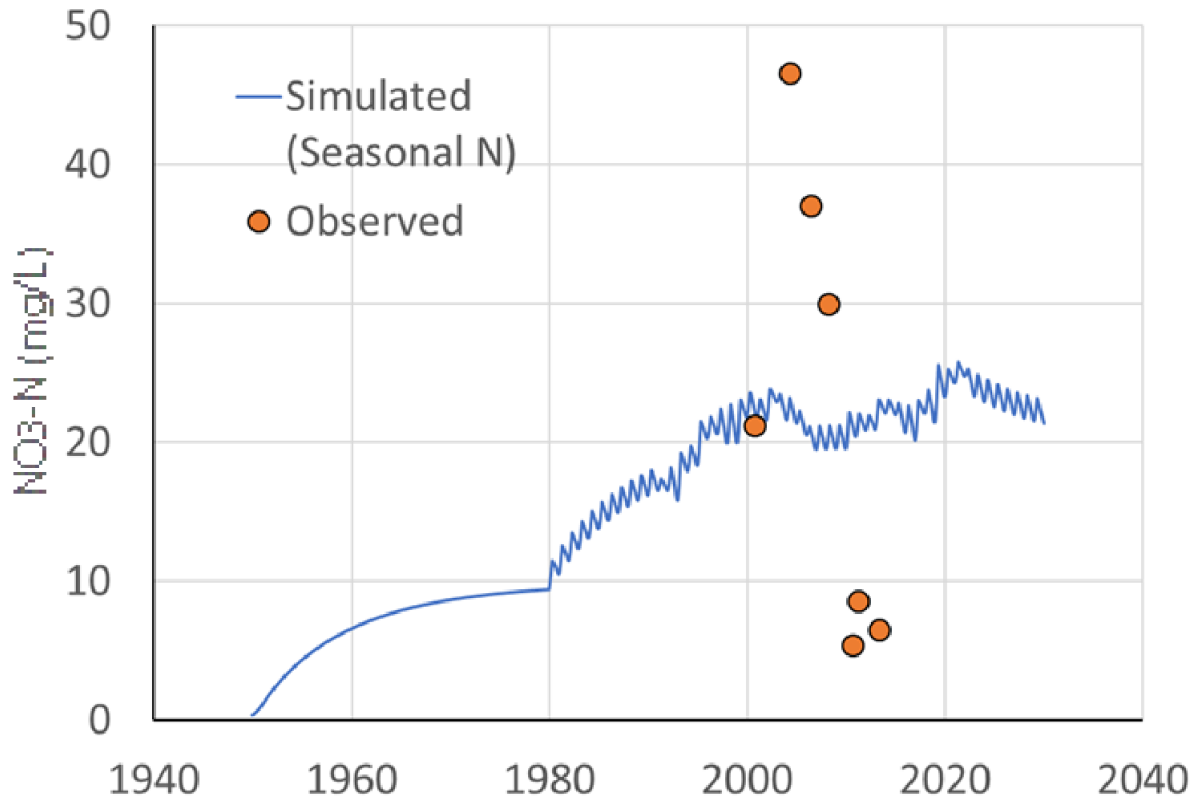


Figure 14 Nitrate-N response in Whiteside County (195-3-80-1370) during variable seasonally applied recharge simulation.

Sensitivity Analysis: Denitrification

We found that assumptions of denitrification were the most important factor when conducting a sensitivity analysis. Within the subsurface, even the slowest denitrification rates modeled have a pronounced effect on the evolution of nitrate-N concentrations (Figure 15) relative to the base case (no denitrification). Roughly 50% is removed at a minimum and up to 80%+ removal is observed at the fastest rates. It is highly probable that the full spectrum of denitrification rates is observed within the Rock River watershed, and that local rates change seasonally and over longer periods. Because we do not have a priori knowledge of redox conditions spatially and through time, we used a homogeneous, moderate denitrification rate (1625 days) applied to the entire model domain in scenarios in which we

tested the impact of other variables.

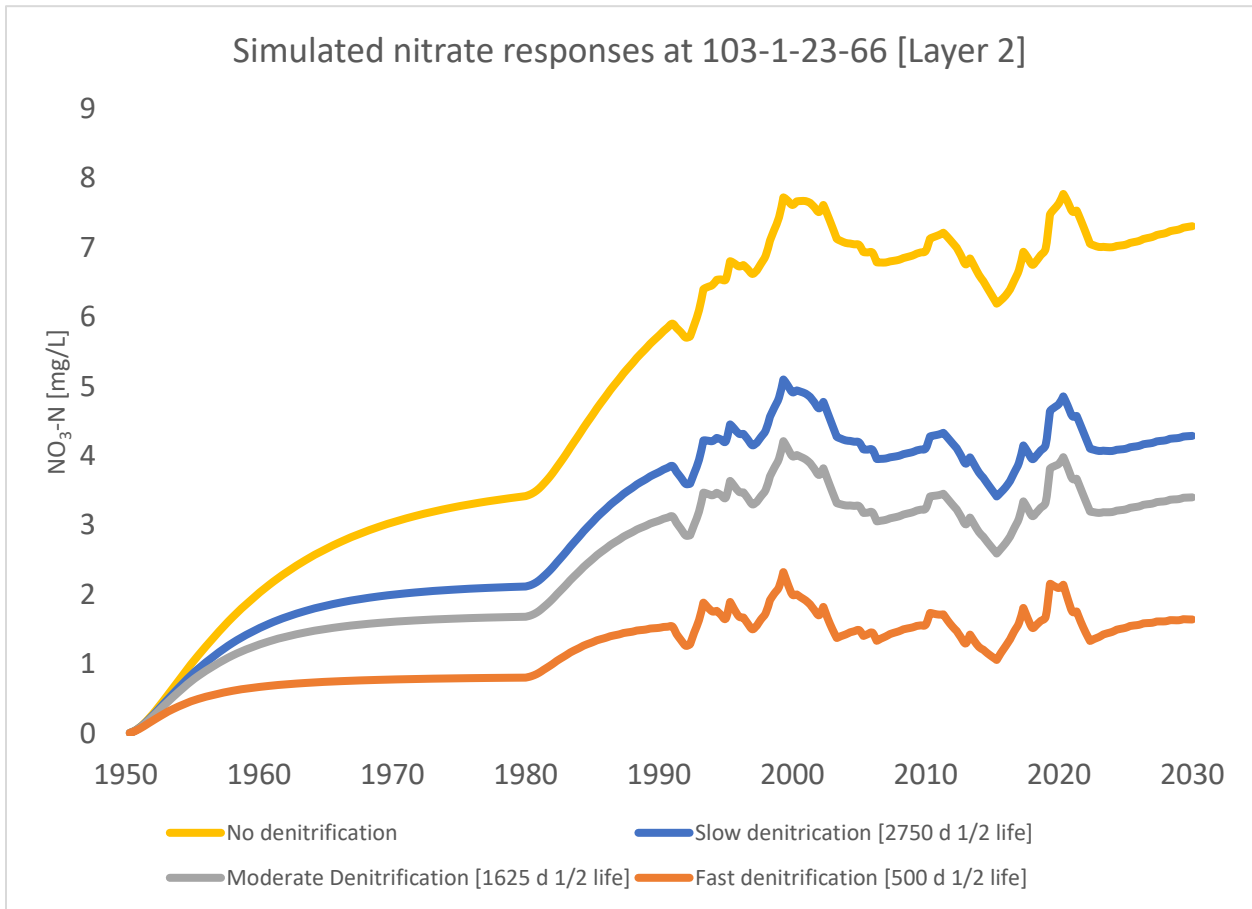


Figure 15 Nitrate-N response in Lee County with varying levels of subsurface denitrification

The observations (Figure 16) are clear; denitrification, whether in-stream or subsurface, is a stronger control on the fate of nitrate (in groundwater) than the presence of artificial drainage. Calibration targets within surficial denitrifying zones saw 50% declines in peak concentrations vs. base case scenarios. This nitrate is presumably unavailable to discharge to the Rock River.

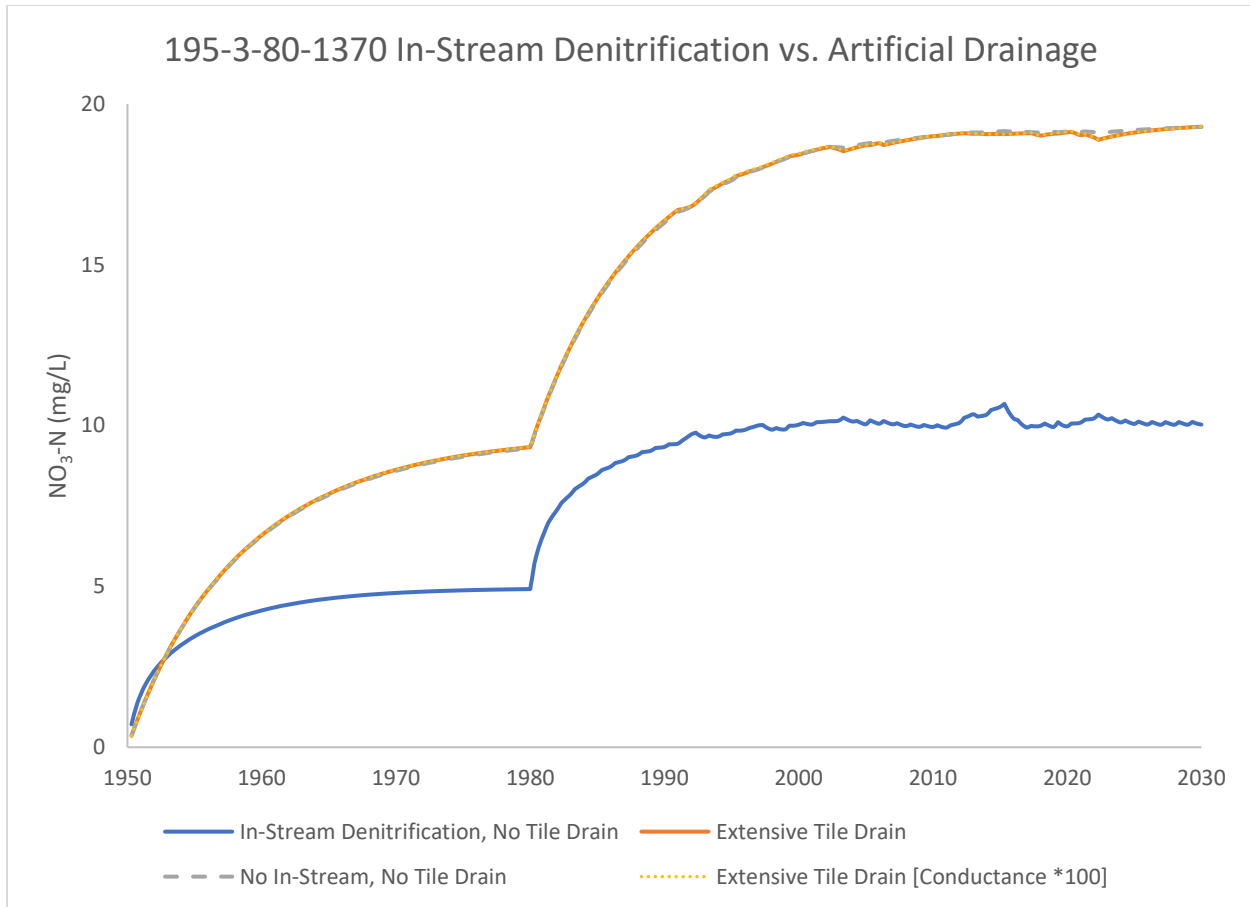


Figure 16 Nitrate-N responses in Whiteside County, comparing the relative impacts of artificial drainage vs in-stream denitrification. Subsurface denitrification rates are assumed to be 1625 days everywhere in the model domain below layer 1.

Interestingly the two variables differ in the timing of their greatest influence in the system. Tile drains uptake more nitrogen during periods of high recharge, because groundwater levels are high enough to interact with drains. In-stream denitrification, however, reduces more nitrogen during periods of lower recharge due to the reduction in flow rates, allowing water to spend more time in reaction zones. Whether denitrification rates are dependent on recharge rates is not considered due to lack of data to fully assess such a phenomenon.

Results: Head, Concentration, and Age Maps

Head map

Figure 17 shows the predevelopment potentiometric surface simulated for the Tampico Aquifer; heads do not vary substantially from this at any point in the simulation. The heads in the Tampico Aquifer drive the flow regime in the shallow, unconfined, portion of this aquifer, with a general flow pattern of east to west south of the Rock River (and more complicated to the north). This regime is interpreted to be oxidizing (resists denitrification), based on analysis of water quality in the GRLMN conducted shortly after the network was established (Burch, 2004).

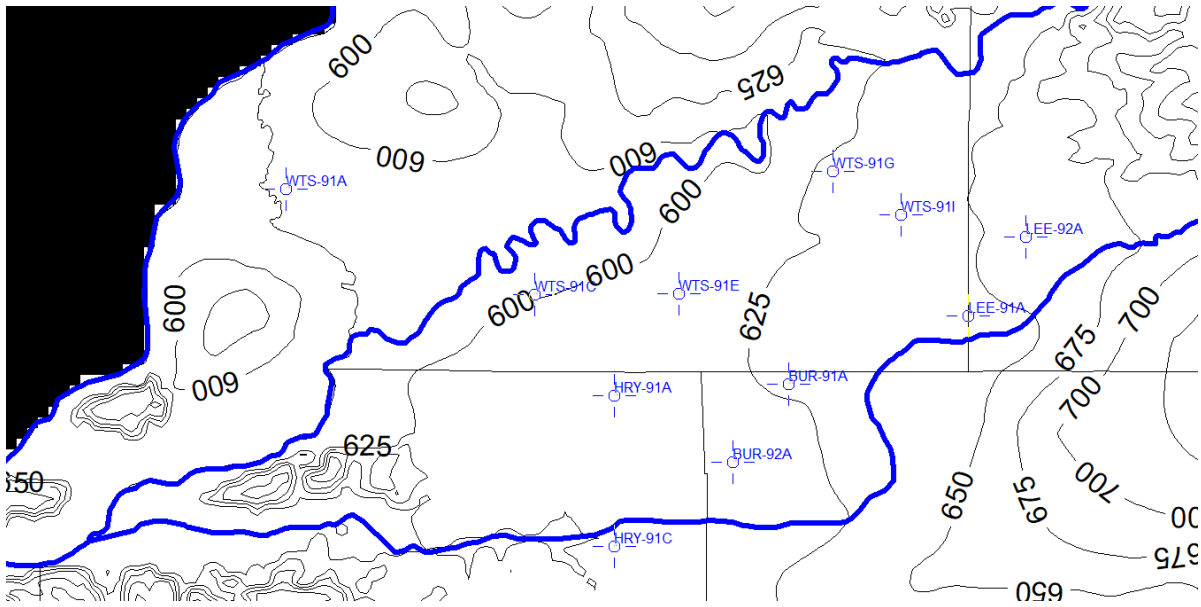


Figure 17 Model generated potentiometric surface for the Tampico Aquifer near the GRLMN. Blue crosshairs symbolize the locations of individual monitoring wells/calibration points.

Discharge zones

Figure 18 shows the vertical flow regime between the topmost layers in the model. Vertical flow is used as a first-order proxy to determine regions of potential discharge and recharge. These zones will change in response to numerous hydrological and hydrogeological variables and extensive field and geophysical investigations are required to verify these simulated results. However, this analysis suggests limited potential for appreciable groundwater discharge given the small geographic extent of discharge and low rates [$< .005$ ft/day].

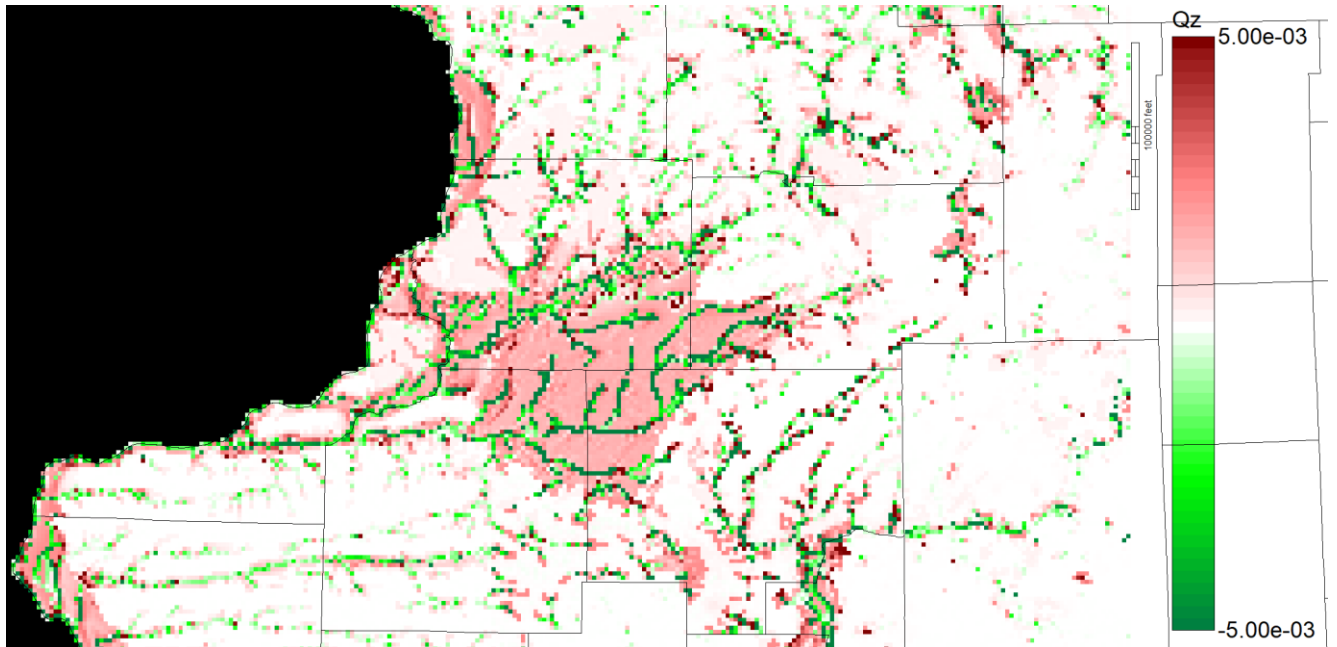


Figure 18 Plot of vertical flow [Qz] in ft/day in layer 2. Regions with negative flow directions [green] are interpreted to be discharge zones, while regions with positive flow directions are interpreted to be regions of aquifer recharge.

The presence of drain tiles, especially if outlets discharge directly into surface water without treatment (Figure 19), provide an additional avenue of discharge, whose contribution to nitrate loads cannot be reliably calculated by the model.



Figure 19 Drain outlet along the Green River, south of Prophetstown. Untreated discharge from fertilized fields can short-circuit denitrification zones and discharge directly into surface water.

Nitrate simulation

Initial nitrate-N concentrations throughout the model domain start at 0 mg/L. At the beginning of each Stress Period all cells in Layer 1 are given a nitrate-N concentration of 10 mg/L, delivered via recharge to the water table, which then moves via advective and diffusive transport through the system throughout the Stress Period. Discussions with Greg McIsaac indicate that this is on the lower end of nitrate-N concentrations measured at tile drain outlets, and therefore a conservative estimate which discounts the nitrate contribution into the system from effluent discharge and livestock operations during the summer months. Nitrate either accumulates in groundwater over time or is removed from the model domain by rivers and streams. For the model results shown here, no denitrification in the aquifer is assumed; this is varied in other simulations and results in reductions in nitrate simulated with depth.

After the first stress period (Figure 20), insufficient time has elapsed to see significant accumulation of nitrate in surficial aquifers. Most applied nitrate in the early Stress Periods is removed from the model by rivers before it can accumulate in groundwater. Some pockets do show infiltration by nitrate, especially in southeast Henry County. These pockets likely coincide with thin, poorly drained or highly permeable surficial sediments. Whatever the case, these pockets of early nitrate arrival are far enough removed from the Rock River that they do not merit consideration here.

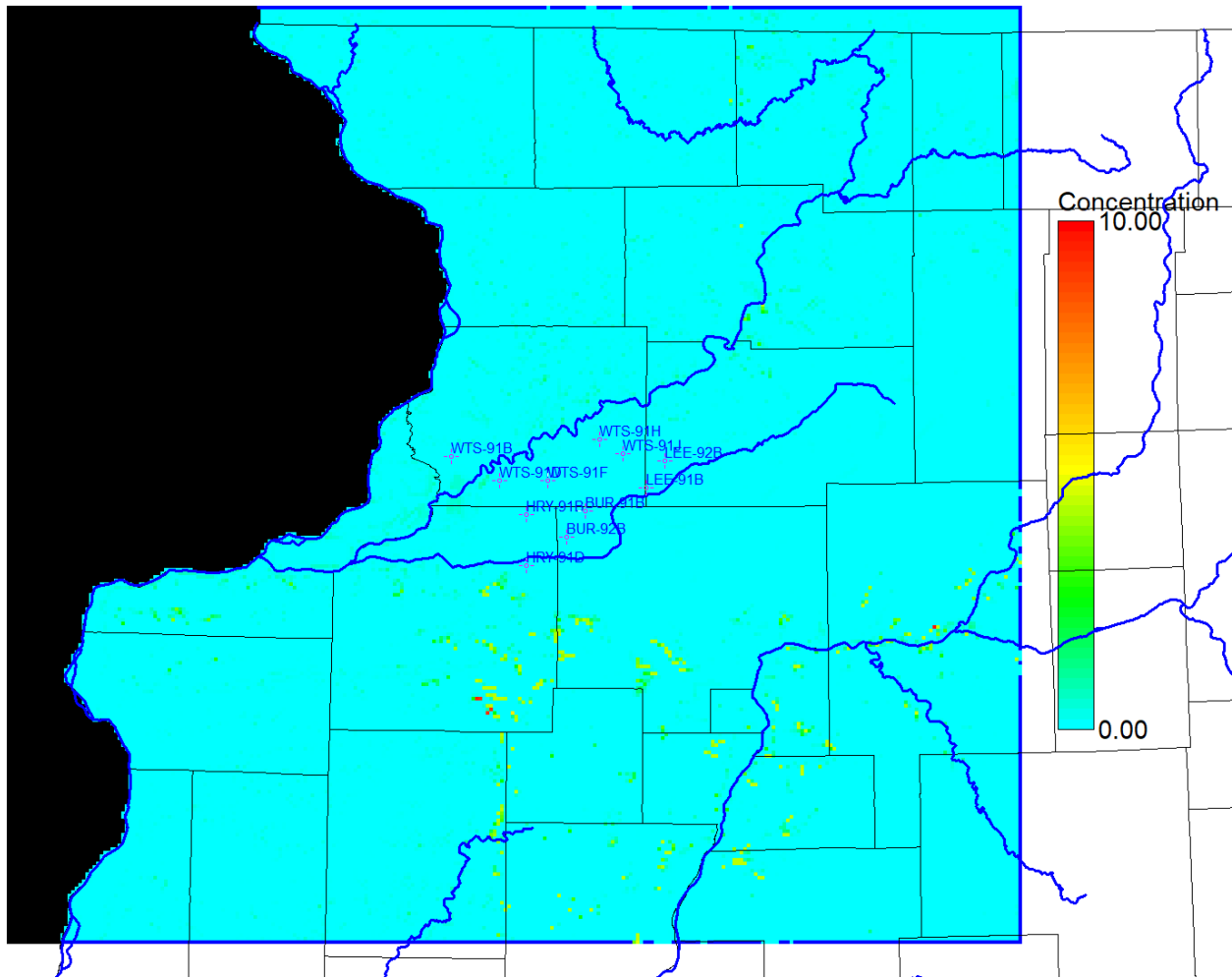


Figure 20 Model generated nitrate-N concentration [mg/L] distribution after Stress Period 1 [1980 non-irrigation], Layer 4 [Tampico aquifer]

By the 50th Stress Period (Figure 21), enough nitrate has infiltrated into groundwater, so that the dominant solute transport pathways in the system are resolvable. It appears that the confining layer between the Tampico and Sankoty aquifers is a significant enough barrier to vertical flow that where it is thickest [NW Bureau and SE Whiteside Counties], nitrate is forced laterally towards the Rock River. This contrasts with the southernmost reaches of the Rock River, where the confining layer is thin, porous, or non-existent, and therefore able to infiltrate deeper and accumulate in groundwater.

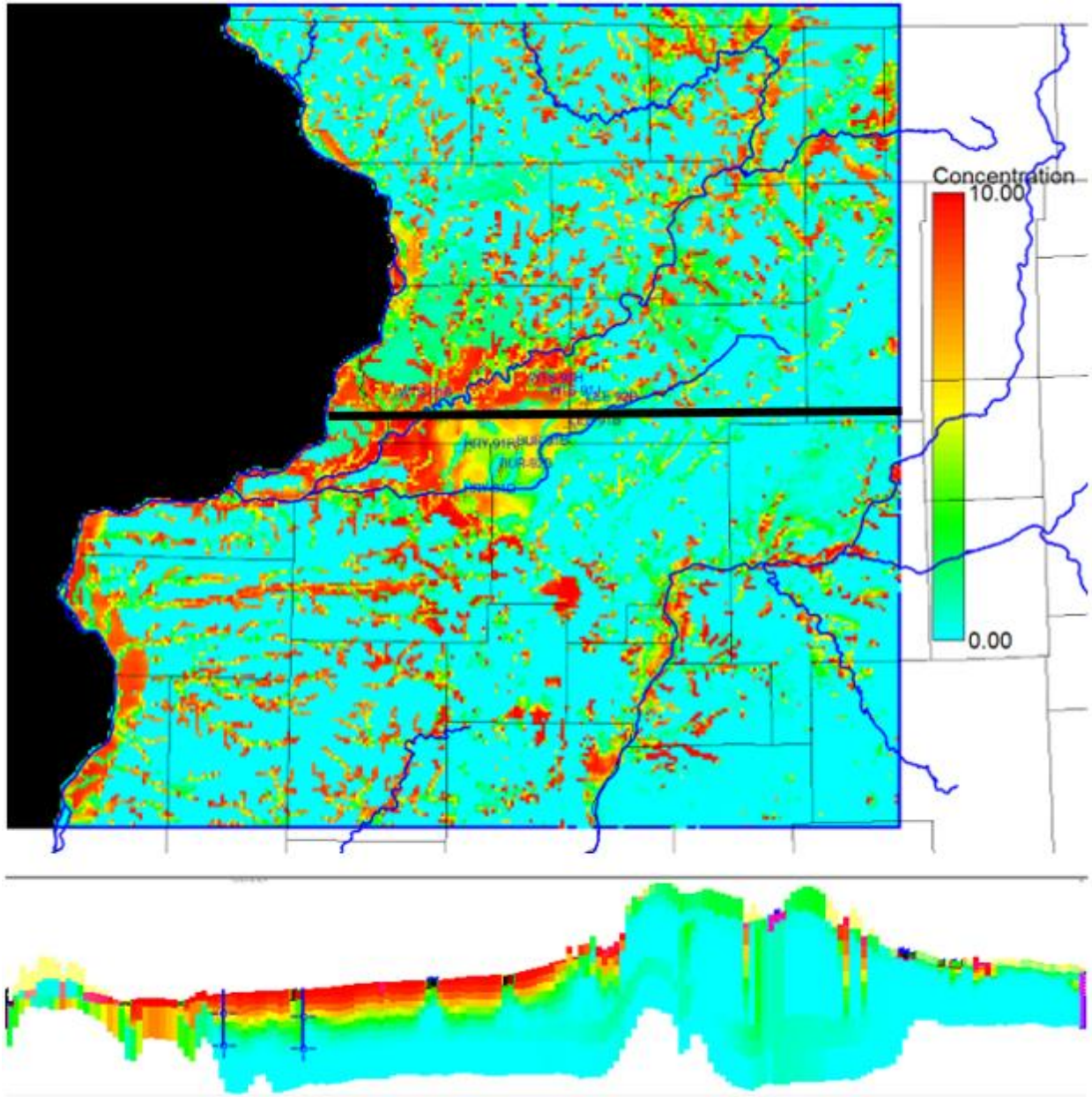


Figure 21 Model generated nitrate-N concentration [mg/L] distribution for Stress Period 50 [2004 irrigation], Layer 4 [Tampico aquifer]. Black line is the location of the bottom cross section.

At the end of the simulation (Figure 22), nitrate-N in the upper, unconfined aquifer has reached equilibrium with the input recharge concentrations and is beginning to infiltrate past the confining layer. Fingerlike zones of low nitrate-N concentrations that drain to the Rock and Green Rivers persist in the upper aquifer. Their locations are likely controlled by local heterogeneities in the geology that cause increased flow and therefore increased delivery of nitrate to streams. One such zone that drains to the Rock River intersects GRLMN monitoring wells WTS-91 E and F but does not intersect nearby WTS-91 C and D. Sampling at these wells would serve as a good “ground truth” for our model observations.

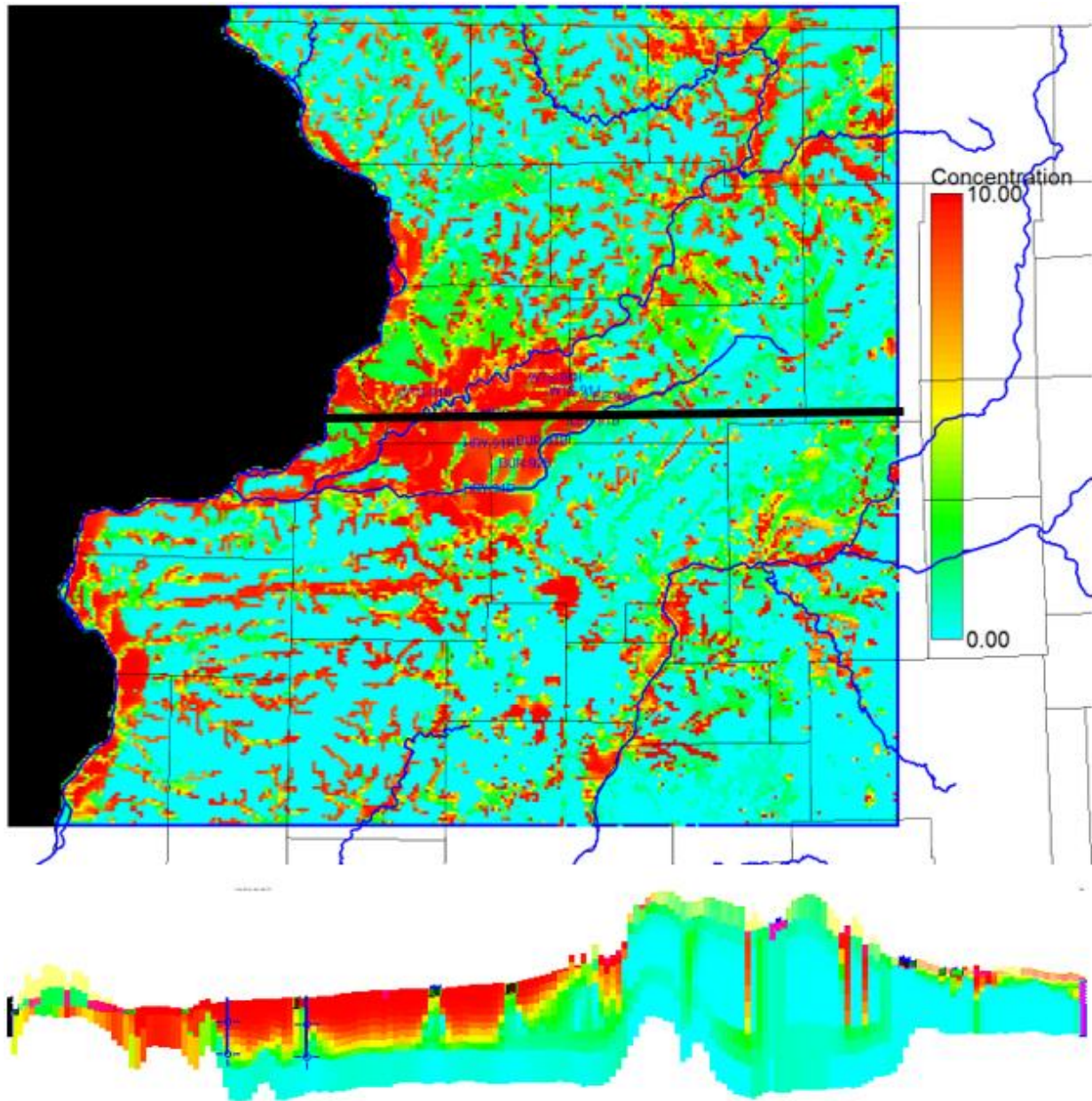


Figure 22 Model generated nitrate-N concentration [mg/L] distribution for Stress Period 101 [2030 non-irrigation], Layer 4 [Tampico aquifer]. Black line is the location of the bottom cross section.

Groundwater age

Groundwater age was calculated by assigning a concentration of zero to the recharge throughout the simulation and calculating a zero-order decay rate of $-1/\text{day}$. This allows all water moving through the aquifer to age by one day for each day of the simulation. For each new stress period, water that just recharged the aquifer will have the youngest age, water that recharged in earlier stress periods will be older, and the oldest water will always be the water that was not removed from the aquifer since the start of the simulation. By the end of the simulation, water can achieve a maximum age of 50 years if it has not discharged to a stream or been pumped by a well.

In general, groundwater age varies with depth, but local geology makes a significant difference in the spatial distribution of age. In the shallow Tampico aquifer, the youngest water occurs between the Rock and Green Rivers, generally coincident with sand and gravel aquifers at land surface (Figure 23) This suggests that the water in the shallow aquifer is more recently recharged. As such, this water is also more vulnerable to contamination. Water in low permeable material has a longer residence time in the aquifer.

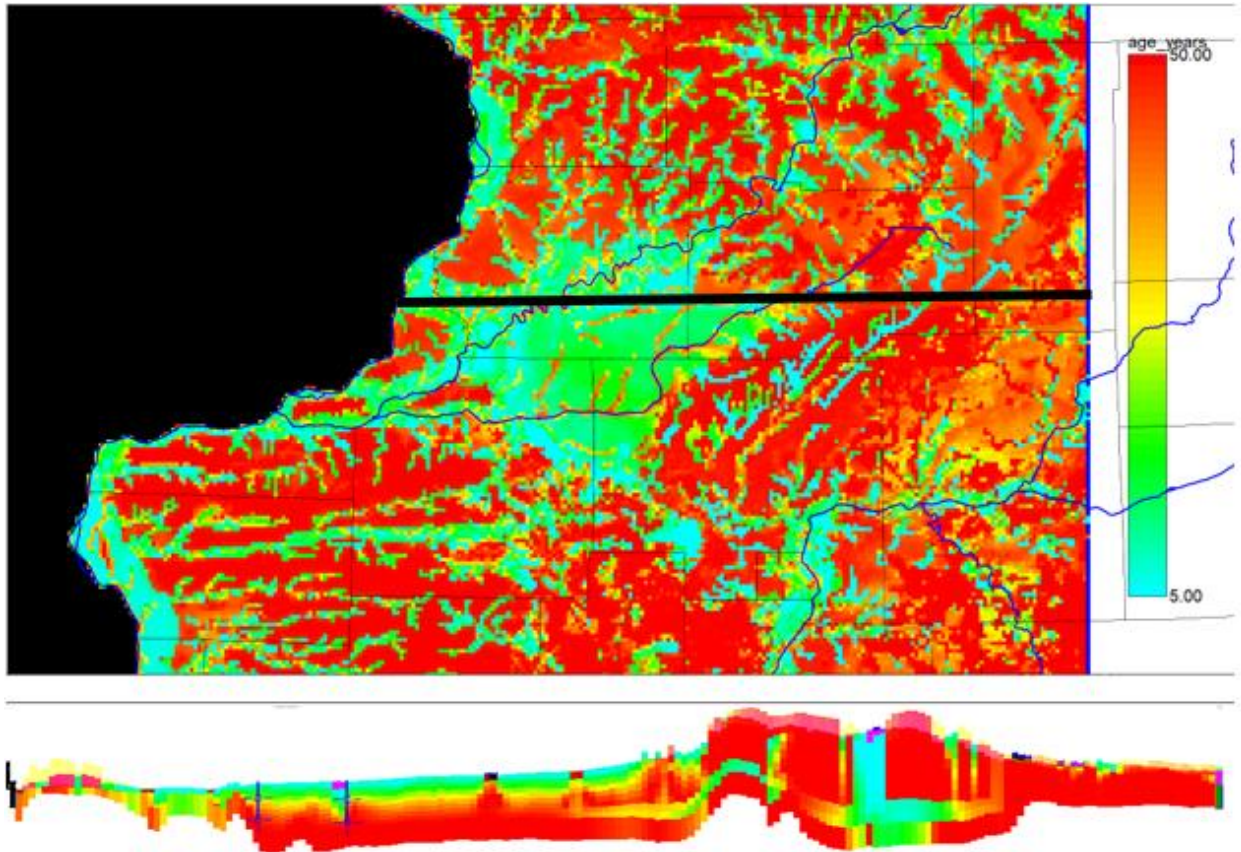


Figure 23 Model generated groundwater age distribution at end of simulation [Stress Period 101], Layer 2. Black line is the location of the bottom cross section. The deepest shade of red represents water that is 50 years of age or older.

In the deeper Sankoty aquifer, except along the Rock River and in local areas of the Green River, groundwater is much older, often greater than 50 years in age (Figure 24). This older water generally would be expected to have lower nitrate-N concentrations, either having been within the aquifer since before agricultural applications or long enough that denitrification has removed nitrate from the aquifer.

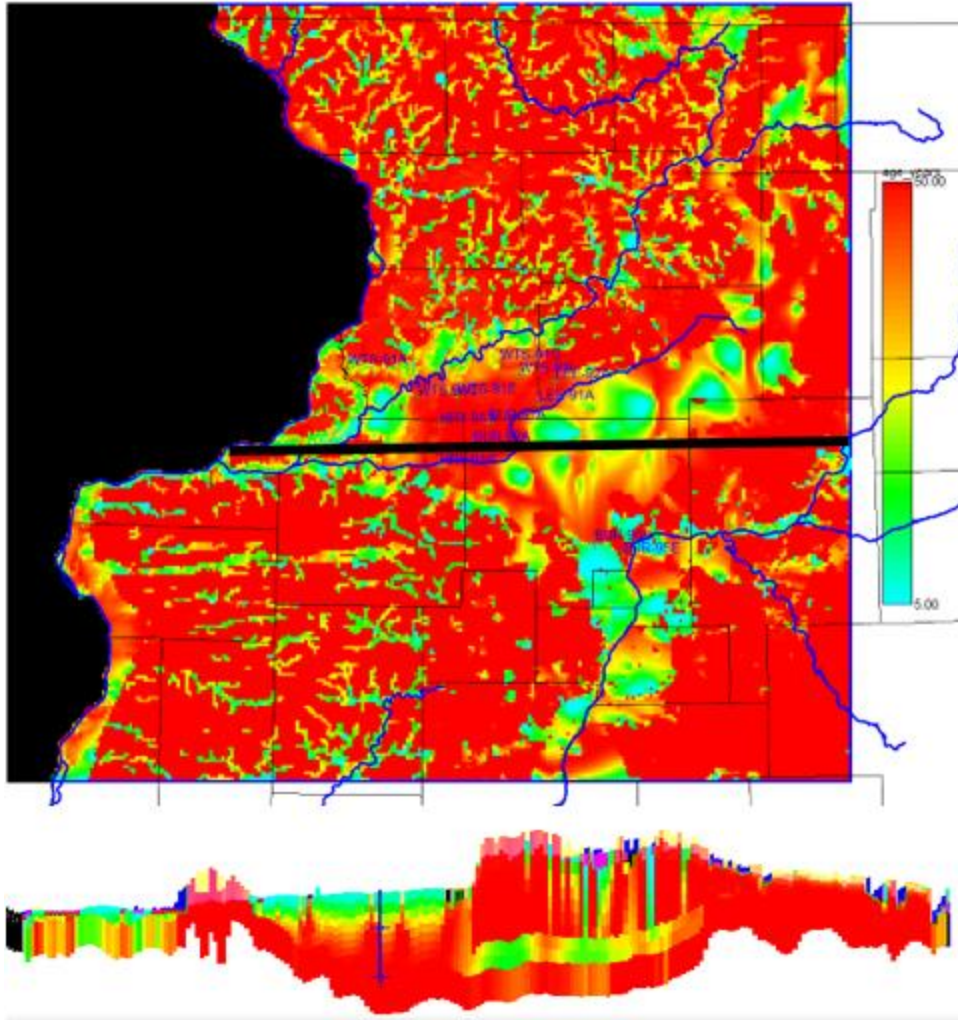


Figure 24 Model generated groundwater age distribution at end of simulation [Stress Period 101], Layer 9. Black line is the location of the bottom cross section.

Calculating Nitrate Loads

Our combined MODFLOW-MT3D model produces both flow and nitrate-N concentration outflows. Our graphical user interface, Groundwater Vistas, allows a user to draw a polygon (Figure 25) over an area and calculate (from the flows and concentrations) a mass loading to rivers. Since rivers in a MODFLOW model can both gain and lose water, we consider the net gain of water (and subsequently nitrate loads) to the river.

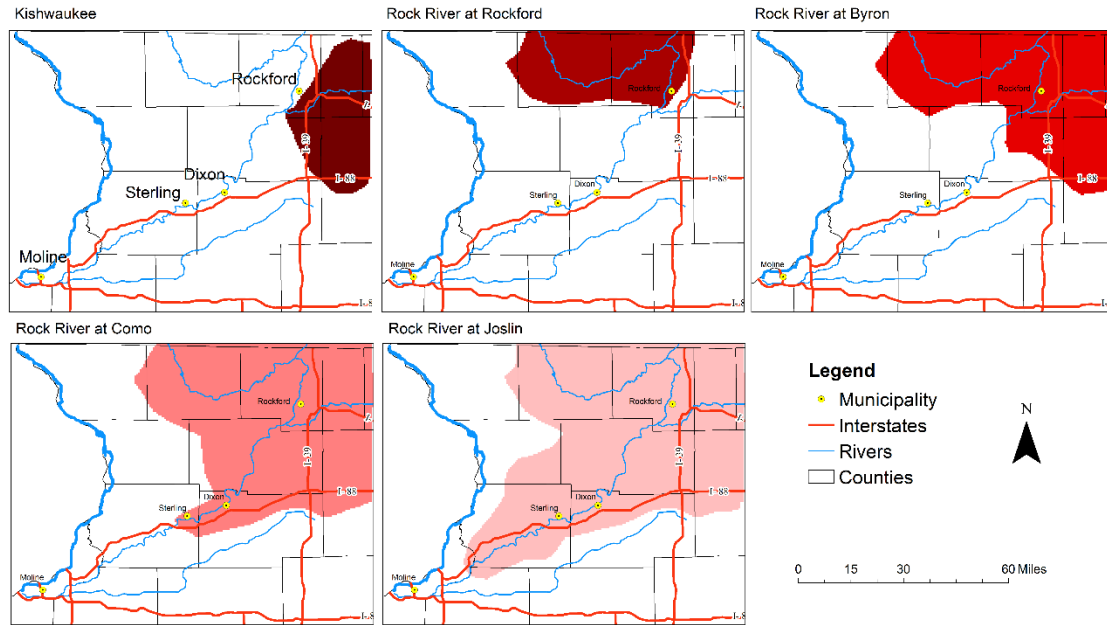


Figure 25 Mass balance polygons used in nitrate load calculations.

While our primary focus was the nitrate that discharged to rivers via groundwater, we also considered drain cells. MODFLOW Drains are similar to rivers, except they can only gain water from the aquifer; they cannot lose water. Mass balance was considered over the entire Rock River Watershed that was simulated (although a few headwaters were outside the model domain), with a particular emphasis on the reach between Rockton and Joslin, which fell completely within the model domain.

Presented in the Table 1 are sample outputs for load calculations for the base model scenario (subsurface denitrification occurs at a 1625-day half-life decay rate, no artificial drainage or in-stream denitrification). Under different assumptions about denitrification

Table 1 Nitrate-N load calculations for base model simulation.

Watershed outlet or section	Nitrate-N load (Mg N/yr)		Change	%Change
	1980	2018		
Rockton	558.04	755.88	+197.84	+35%
Kishwaukee	1153.70	1391.57	+237.87	+20%
Rockford	766.50	987.71	+221.21	+30%
Byron	2111.71	2609.58	+497.87	+25%
Como	3027.85	3730.49	+702.64	+25%
Joslin	3659.60	3916.98	+257.38	+10%

An attempt was made to replicate the approximately 5000 Mg N/yr surplus load at Joslin proposed to be from groundwater contributions (Mclsaac, 2019) by tripling the nitrate-N input concentrations and disregarding the effects of denitrification or trying to match observed data.

While this simulation (Table 2) comes closer to the proposed value, nitrate-N inputs at these levels (30 mg/L non-agricultural, 60 mg/L agricultural) will certainly result in noticeable impacts to public health, particularly in infants (Walton, 1951), and likely exceed the fertilizer requirements of crops in this region.

Table 2 Nitrate-N load calculations for model simulation in which nitrate-N inputs were tripled.

Watershed outlet or section	Nitrate-N load (Mg N/yr)		Change	%Change
	1980	2018		
Joslin	13234.03	17121.53	+3887.50	+30%

Additionally, even this unrealistic nitrate-N input fails to account for anomalously high reported concentrations in some IDOA wells (Figure 26). This suggests the potential for highly localized sources of contamination that are on finer scales than the model resolution can detect. Furthermore, the observed rapid declines after 2004 cannot be simulated by varying application rates. Local denitrification is the variable best suited to vary to match the observed swing. Assuming no net nitrate entered the system after 2004, a 6-year denitrification half-life (~2200 days) is sufficient to model the observed decline at monitoring well 195-3-80-1370.

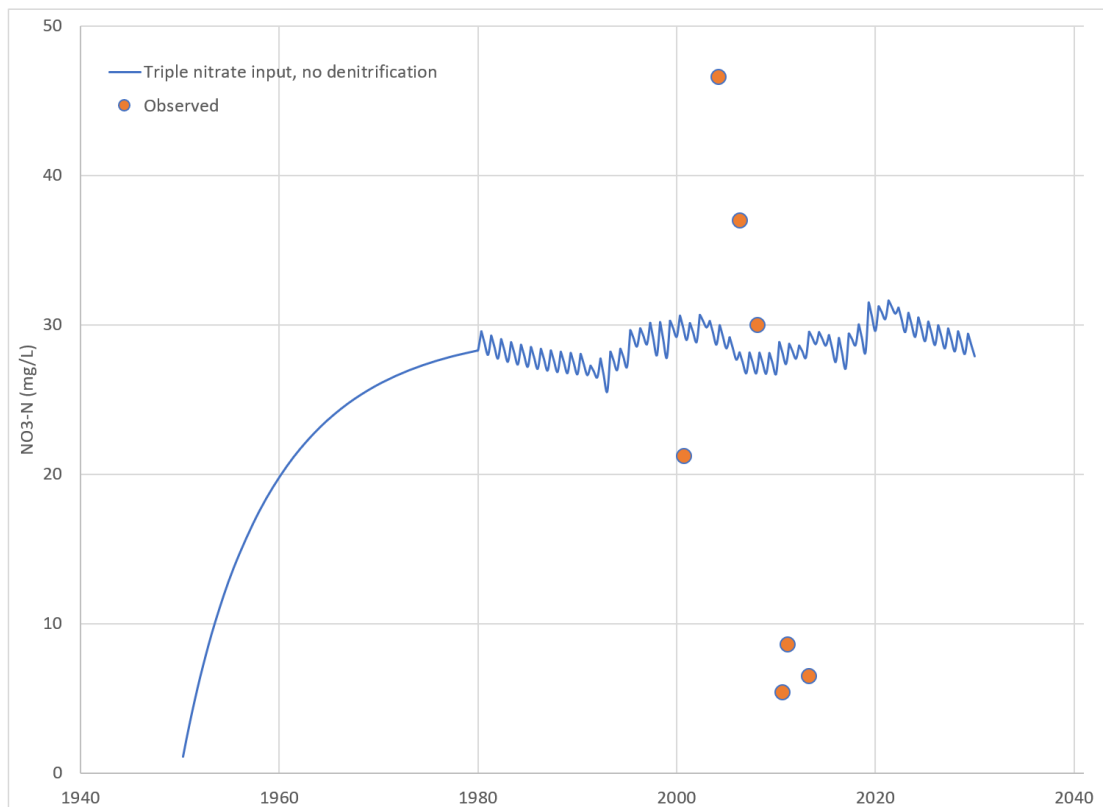


Figure 26 Nitrate-N response in Whiteside County (195-3-80-1370) during variable seasonally applied recharge simulation with triple nitrate-N inputs compared to baseline (Figure 14).

Future Directions

At this stage it can be stated that the groundwater contribution to nitrate loads in the Rock River has certainly increased, very slightly, over the past 50 years. However, it does not appear to be the major contributor of the total observed load increases throughout the watershed. More work remains to ascertain the true proportion of groundwater's relative contribution, but nearly flat hydraulic gradients in the major groundwater reservoir (long residence times) underlying the Rock River, coupled with the supposition of at least some subsurface denitrification, imply that this result cannot change much without the assumption of unrealistic historic or current inputs.

Although increased nitrate loads to the Rock River cannot be wholly explained by legacy contributions from groundwater, it does play an important role in its transport/remediation. Conveyance through reducing conditions in the subsurface allows for relatively quick removal, relative to flow rates, through denitrification. An additional denitrification buffer exists in the organic-rich zones near and within streams. A dedicated sampling campaign that not only considers nitrate-N concentrations seasonally but also redox conditions at depth would go a long way in refining this simulation.

More consideration should be paid to the role of artificial drainage in the region. Although drain tiles are important for protecting crop yields, they provide a route for runoff to circumvent subsurface or near-stream denitrification. Other studies (Schilling et al., 2012) have shown the importance of subsurface drainage in "exponentially decreasing groundwater transit times", depending on drainage densities and incision depths. The spatial and temporal resolutions of the current model are too large, and centralized knowledge of regional drainage infrastructure does not exist to adequately simulate this variable and calculate its relative contribution to increased loads. Further refinement to the model to address this will likely not be possible without buy-in from agricultural stakeholders.

Guidance from the agricultural community should also be sought in refining water demand, methods of conveyance and fertilizer practices. The last comprehensive study on irrigation practices in Illinois by ISWS was over 30 years ago (Bowman & Kimpel, 1991). An update, with an additional focus on drainage and fertilizer practices would enrich this study and any other inquiry into this region's hydrology and hydrogeology.

Finally, additional investment in improving the model resolution will result in a valuable water supply planning tool for the region. Proposed management strategies can be set-up and assessed within hours, and should new contaminants of concern become identified, their ecological impacts and transport fate can be quickly ascertained, and effective remediation strategies can be proposed.

Acknowledgments

This report was funded by the Illinois Environmental Protection Agency. The views expressed herein are those of the authors and do not necessarily reflect the views of the sponsor or the Illinois State Water Survey.

Many people contributed to the successful completion of this project. Devin Mannix was instrumental in locating historic water quality data for the region as well as assisting in developing model scenarios that addresses the role of artificial drainage. Mike Krasowski provided GIS support in creating figures and

provided technical advice on methodologies to simulate recharge. Greg McIsaac (UIUC NRES Professor Emeritus) and Trevor Sample (IEPA) provided helpful review comments and advice throughout the project period.

A special thanks to Illinois Natural Resources Conservation Service, Illinois Corn Growers Association, Illinois Farm Bureau, Blackhawk Hills Regional Council, and the Illinois Groundwater Association for providing platforms to disseminate preliminary and final results to, and hold discussions with, regional stakeholders.

References

- Abrams, D. B., Mannix, D. H., Hadley, D. R., & Roadcap, G. S. (2018). *Groundwater Flow Models of Illinois: Data, Processes, Model Performance, and Key Results*. Illinois State Water Survey. Retrieved from <https://www.ideals.illinois.edu/handle/2142/102968>
- Bowman, J. A., & Kimpel, B. C. (1991). Irrigation Practices in Illinois. *ISWS RR-118*. Retrieved from <https://hdl.handle.net/2142/75854>
- Burch, S. L. (2004). *Groundwater Conditions of the Principal Aquifers of Lee, Whiteside, Bureau, and Henry Counties, Illinois* (Data/Case Study No. 1) (p. 97). Champaign, IL: Illinois State Water Survey. Retrieved from <https://www.ideals.illinois.edu/handle/2142/74884>
- Forshay, K. J., & Stanley, E. H. (2005). Rapid Nitrate Loss and Denitrification in a Temperate River Floodplain. *Biogeochemistry*, 75(1), 43–64. <https://doi.org/10.1007/s10533-004-6016-4>
- Kelly, W. R., & Ray, C. (1999). Impact of Irrigation on the Dynamics of Nitrate Movement in a Shallow Sand Aquifer a.
- Kuehner, K., Dogwiler, T., & Kjaersgaard, J. (2016). Examination of Soil Water Nitrate-N Concentrations from Common Land Covers and Cropping Systems in Southeast Minnesota Karst. *Minnesota Department of Agriculture*. Retrieved from <https://wrl.mnpals.net/islandora/object/WRLrepository%3A3654/datastream/PDF/view>
- Lin, J., Böhlke, J. K., Huang, S., Gonzalez-Meler, M., & Sturchio, N. C. (2019). Seasonality of nitrate sources and isotopic composition in the Upper Illinois River. *Journal of Hydrology*, 568, 849–861. <https://doi.org/10.1016/j.jhydrol.2018.11.043>
- Mclsaac, G. (2019). *Nitrate and Total Phosphorus Loads in Illinois Rivers: Update Through the 2017 Water Year* (p. 68). Illinois Environmental Protection Agency.

- Puckett, L. J., Tesoriero, A. J., & Dubrovsky, N. M. (2011). Nitrogen Contamination of Surficial Aquifers—
A Growing Legacy. *Environmental Science & Technology*, 45(3), 839–844.
<https://doi.org/10.1021/es1038358>
- Schilling, K. E., Jindal, P., Basu, N. B., & Helmers, M. J. (2012). Impact of artificial subsurface drainage on
groundwater travel times and baseflow discharge in an agricultural watershed, Iowa (USA):
IMPACT OF DRAINAGE TILES ON GROUNDWATER TRAVEL TIMES. *Hydrological Processes*, 26(20),
3092–3100. <https://doi.org/10.1002/hyp.8337>
- Uffink, G. (2003). Determination of denitrification parameters in deep groundwater. *RIVM*, 76.
- Valayamkunnath, P., Barlage, M., Chen, F., Gochis, D. J., & Franz, K. J. (2020). Mapping of 30-meter
resolution tile-drained croplands using a geospatial modeling approach. *Scientific Data*, 7(1),
257. <https://doi.org/10.1038/s41597-020-00596-x>
- Walton, G. (1951). Survey of Literature Relating to Infant Methemoglobinemia Due to Nitrate-
Contaminated Water. *American Journal of Public Health and the Nations Health*, 41(8_Pt_1),
986–996. https://doi.org/10.2105/AJPH.41.8_Pt_1.986
- Watkins, J., Rasmussen, N., Johnson, G., Streitz, A., & Ahmad, K. (2013, September). Nitrate-Nitrogen in
the Springs and Trout Streams of Southeast Minnesota. Newsletter.
- Worthen, A. H. (1866). Geological survey of Illinois., (8v.), 8v.